Accepted Manuscript

Development of novel bis-pyrazole derivatives as antitumor agents with potent apoptosis induction effects and DNA damage

Hong Dai, Shushan Ge, Jin Guo, Shi Chen, Meiling Huang, Jiaying Yang, Siyu Sun, Yujun Shi, Yong Ling

PII: S0223-5234(17)31001-2

DOI: 10.1016/j.ejmech.2017.11.098

Reference: EJMECH 9973

To appear in: *European Journal of Medicinal Chemistry*

Received Date: 22 October 2017

Revised Date: 27 November 2017

Accepted Date: 29 November 2017

Please cite this article as: H. Dai, S. Ge, J. Guo, S. Chen, M. Huang, J. Yang, S. Sun, Y. Shi, Y. Ling, Development of novel bis-pyrazole derivatives as antitumor agents with potent apoptosis induction effects and DNA damage, *European Journal of Medicinal Chemistry* (2018), doi: 10.1016/j.ejmech.2017.11.098.

Development of novel bis-pyrazole derivatives as antitumor agents with potent apoptosis induction effects and DNA damage

Hong Dai [a,b], Shushan Ge [a,b], Jin Guo [b,c], Shi Chen [b,c], Meiling Huang [b], Jiaying Yang [b], Siyu Sun [a], Yujun Shi [a,*], and Yong Ling [a,b,c,*]

[a] College of Chemistry and Chemical Engineering, Nantong University, Nantong 226019, People's Republic of China

[b] School of Pharmacy, Nantong University, Nantong 226001, People's Republic of China

[c] Jiangsu Province Key Laboratory for Inflammation and Molecular Drug Target, Nantong University, Nantong 226001, China.

Graph Abstract:

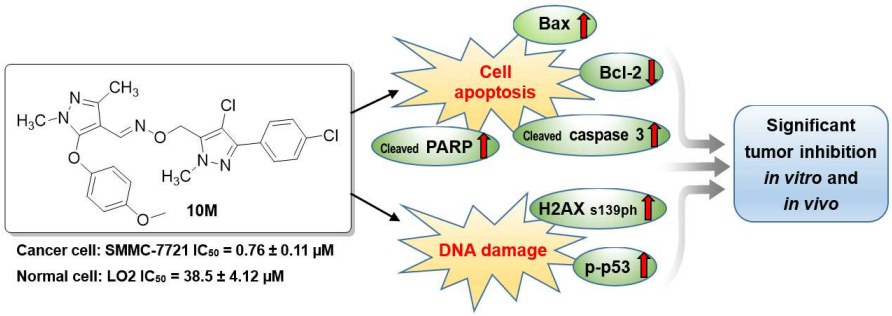

ELSEVIER

European Journal of Medicinal Chemistry
journal homepage: www.elsevier.com

Development of novel bis-pyrazole derivatives as antitumor agents with potent apoptosis induction effects and DNA damage

Hong Dai [a,b], Shushan Ge [a,b], Jing Guo [b,c], Shi Chen [b,c], Meiling Huang [b], Jiaying Yang [b], Siyu Sun [a], Yujun Shi [a,*], Yong Ling [a,b,c,*]

[a] College of Chemistry and Chemical Engineering, Nantong University, Nantong 226019, People's Republic of China
[b] School of Pharmacy, Nantong University, Nantong 226001, People's Republic of China
[c] Jiangsu Province Key Laboratory for Inflammation and Molecular Drug Target, Nantong University, Nantong 226001, China.

ARTICLE INFO

Article history:
Received
Received in revised form
Accepted
Available online

Keywords:
Synthesis
Antitumor agent
Bis-pyrazole derivatives
Apoptosis
DNA damage

ABSTRACT

A series of bis-pyrazole derivatives were designed and synthesized, and their antitumor effects *in vitro* and *in vivo* were investigated. Several compounds displayed good antiproliferative activity with IC_{50} values in low-micromolar range against three human cancer cell lines *in vitro*, superior to 5-FU. The most potent compound **10M** selectively inhibited human hepatocellular carcinoma cells but not non-tumor liver cell proliferation *in vitro*, and significantly triggered SMMC-7721 cell apoptosis by cleavage of both PARP and caspase-3 in a concentration-dependent manner. Further study revealed that the potent activity in the cell growth inhibition and apoptosis induction effects of **10M** were related to DNA damage and activation of the p53 signaling pathway. Moreover, **10M** showed low acute toxicity to mice and significant growth inhibition of the hepatoma tumor *in vivo*.

1. Introduction

Like as energy and environmental crisis, cancer has become one of the most important things which people living on earth have to face today [1]. Although great efforts from worldwide researchers have been devoted in this field, the mechanism and treatment method of cancer remain very limited. Chemotherapy has established a new era of molecularly targeted therapeutics, the efficacy of existing drugs for the treatment of cancers is rather limited [2], and it is necessary to develop potent and effective novel therapeutic agents to overcome limitations of current therapy including the development of drug resistance.

For their fruitful applications in pharmaceutical and agrochemical fields, heterocyclic compounds have built a reputation in bioactive molecules [3]. The majority of anticancer drugs currently used in clinical are derived from heterocyclic compounds [4-6]. As an important branch of heterocycles, pyrazole have been widely involved in the development of various bioactive molecules such as antibacterial, anti-inflammatory, antifungal, antiviral, and antimicrobial agents [7-16]. Apart from that, pyrazole-containing compounds also show great potentials to be used as anticancer agents. As shown in Fig. 1, pyrazole-containing compounds **a** and **b** synthesized by Ganga et al [17] exhibit good growth inhibitory activities against MIAPaCa-2, MCF-7 and HeLa human cancer cell lines. Effective anti-proliferative activities against human lung cancer cell lines A549 has been observed by Sun et al [18] for compound **c**. Hassan and the coworkers [19] had reported the wonderful bioactivities to colorectal cancer HCT116 and prostate adenocarcinoma PC-3 human cancer cell lines of compounds **d** and **e**. Ding et al [20] also reported a significant effect of compound **f** to promote cell apoptosis with an IC_{50} value of 15.22 μM.

Among various pyrazole derivatives, pyrazole oxime compounds have shown broad spectrum of antitumor, antibacterial, insecticidal, antimicrobial, and antifungal activities and attracted increasing attention [21-32]. For instance, Park et al [33] reported an excellent pyrazole oxime lead compound **g** (Fig. 1) delivering potential antitumor activities against XF498 and HCT15, with IC_{50} values of 0.02 and 0.01 μg/mL, respectively. Stronger anti-colonic carcinoma activities superior to 5-FU and cisplatin have also been found in our previously studies with pyrazole oxime derivatives bearing a 1,2,3-thiadiazole moiety [34]. Recently, Gomha [35] indicated that increasing the number of pyrazole rings in the molecule structure can be in favor of their bioactivities. On the basis of above-mentioned cases, incorporating substituted pyrazole groups with pyrazole oximes to form novel bis-pyrazole derivatives would facilitate its further enhancement of anticancer activity. We herein report the design and syntheses of a series of novel bis-pyrazole derivatives (**10a–n** and

* Corresponding author. Tel.: +86-513-85051892; fax: +86-513-85051892; e-mail: Lyyy111@sina.com, yjshi2015@163.com.

10A-N), as well as the investigation on their *in vitro* and *in vivo* antitumor activities, selectivity, and apoptotic mechanism in human carcinoma cell lines.

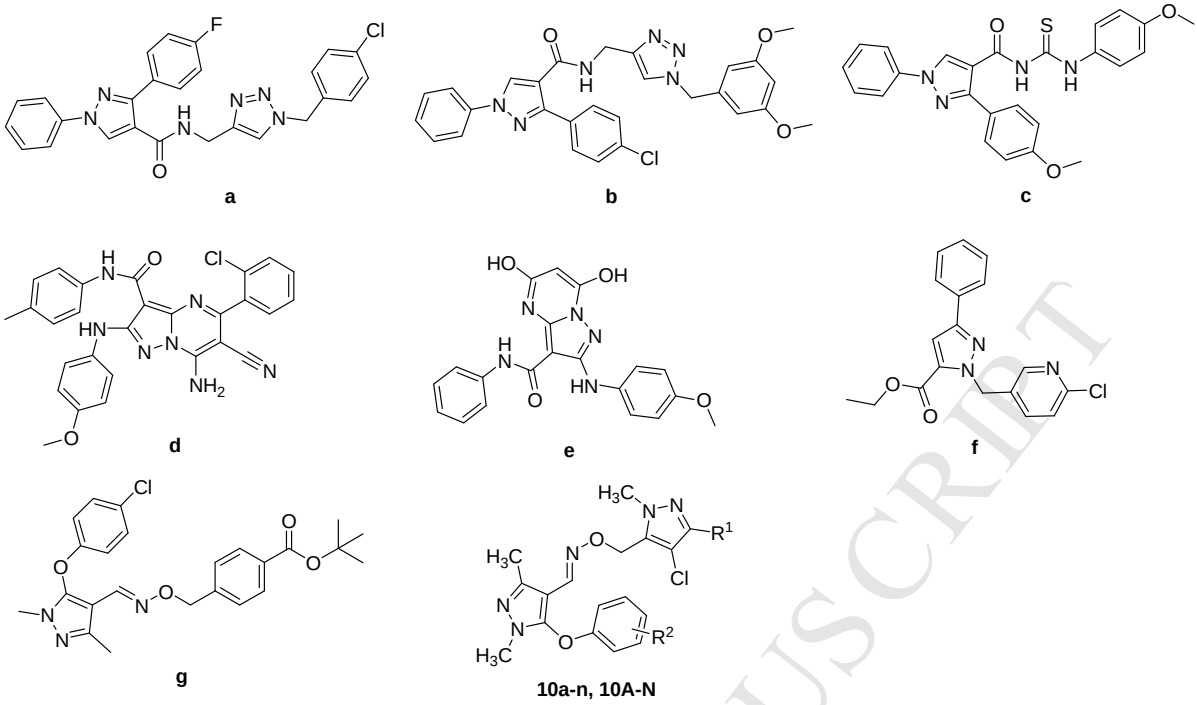

Fig. 1. Chemical structures of pyrazole derivatives **a~g** as antitumor agents and new designed compounds **10a–n** and **10A-N**.

2. Results and discussions

2.1. Chemistry

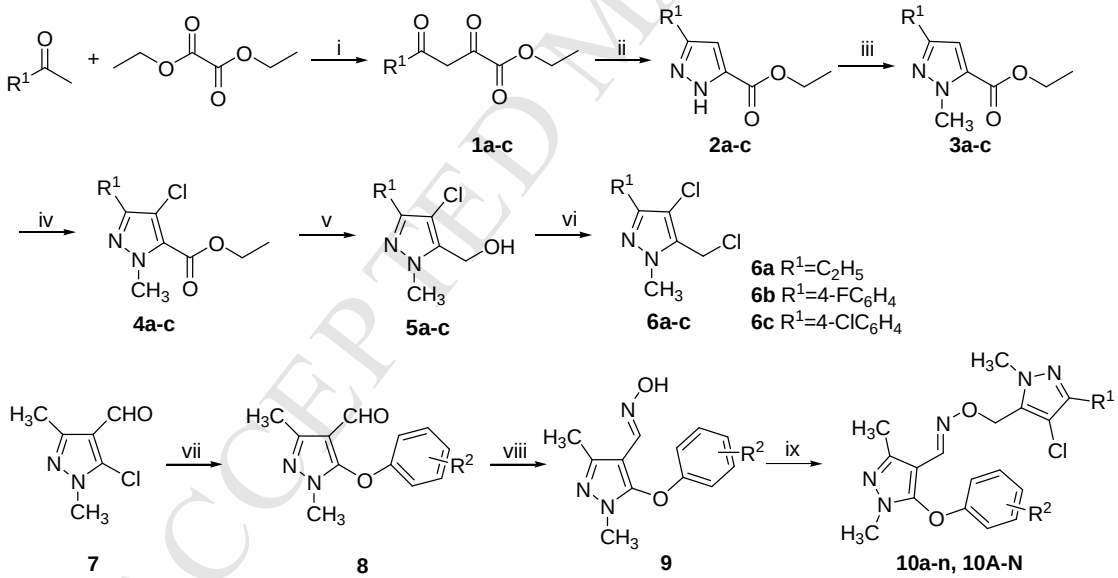

Compd.	R^1	R^2	Compd.	R^1	R^2
10a	C_2H_5	4-F	**10A**	4-FC_6H_4	4-F
10b	C_2H_5	2-F	**10B**	4-FC_6H_4	4-Cl
10c	C_2H_5	4-Cl	**10C**	4-FC_6H_4	4-Br
10d	C_2H_5	3-Cl	**10D**	4-FC_6H_4	4-I
10e	C_2H_5	2-Cl	**10E**	4-FC_6H_4	4-CH_3
10f	C_2H_5	4-Br	**10F**	4-FC_6H_4	4-OCH_3
10g	C_2H_5	4-I	**10G**	4-FC_6H_4	4-OCF_3
10h	C_2H_5	4-CH_3	**10H**	4-ClC_6H_4	4-F
10i	C_2H_5	3-CH_3	**10I**	4-ClC_6H_4	4-Cl
10j	C_2H_5	2-CH_3	**10J**	4-ClC_6H_4	4-Br

10k	C_2H_5	4-OCH_3	**10K**	4-ClC_6H_4	4-I
10l	C_2H_5	2-OCH_3	**10L**	4-ClC_6H_4	4-CH_3
10m	C_2H_5	4-OCF_3	**10M**	4-ClC_6H_4	4-OCH_3
10n	C_2H_5	2-OCF_3	**10N**	4-ClC_6H_4	4-OCF_3

Scheme 1. General procedure for the synthesis of compounds **10a-n** and **10A-N**. Reagents and conditions: (i) EtONa, EtOH, 0 □,12 h, 72-80%; (ii) hydrazine hydrate, HOAc, EtOH, rt, 12 h, or 80% hydrazine hydrate, concentrated hydrochloric acid, EtOH, 85 □, 5-8 h, 65-70%; (iii) Me_2SO_4, Na_2CO_3, CH_2Cl_2, reflux, 24 h, 68-75%; (iv) SO_2Cl_2, $ClCH_2CH_2Cl$, reflux, 4 h, 75-83%; (v) $LiAlH_4$, THF, 0 □, 1 h, 63-69%; (vi) $SOCl_2$, CH_2Cl_2, 0 □, 20 min, rt, 1 h, 55-62%; (vii) substituted phenols, NaOH, EtOH, reflux, 2-3 h, DMSO, 105 □, 10-18 h, 56-71%; (viii) hydroxylamine hydrochloride, KOH, MeOH, reflux, 6-17 h, 59-68%; (ix) compounds **6a-6c**, K_2CO_3, Cs_2CO_3, MeCN, reflux, 12-18 h, 75-86%.

The synthetic route for the target compounds **10a-n** and **10A-N** was summarized in Scheme 1. Claisen condensation of different substituted ketones with diethyl oxalate afforded ethyl 2,4-dioxo substituted butanoates **1a-c**, which were further reacted with hydrazine to obtain ethyl 3-phenyl-1*H*-pyrazole-5-carboxylates **2a-c** [36]. Compounds **2a-c** were treated with dimethyl sulfate to afford ethyl 1-methyl-3-ethyl(or aryl)-1*H*-pyrazole-5-carboxylates **3a-c**. Then the reaction of compounds **3a-c** with sulfuryl chloride gave compounds **4a-c** conveniently, which were transformed into intermediates **5a-c** by the addition of $LiAlH_4$. The reaction of compounds **5a-c** with thionyl chloride produced the key intermediates **6a-c**. Meanwhile, the condensation of 1-methyl-3-methyl-5-chloro-1*H*-pyrazole-4-carbaldehyde **7** [37] with various substituted phenols under basic condition to form 1-methyl-3-methyl-5-aryloxy-1*H*-pyrazole-4-carbaldehyde **8**. Intermediate **8** was reacted with hydroxylamine hydrochloride under basic condition to provide 1-methyl-3-methyl-5-aryloxy-1*H*-pyrazole-4-carbaldehyde oxime **9** [38]. Finally, compound **9** and the key intermediates **6** were mixed in acetonitrile and heated to reflux for 12-18 h using potassium carbonate as alkali and cesium carbonate as catalyst, and a series of novel bis-pyrazole derivatives **10a-n** and **10A-N** were obtained in good yields.

*2.2. MTT assay of compounds **10a-n** and **10A-N***

All the synthesized compounds **10a-n** and **10A-N** were preliminarily screened for their cancer cell growth inhibitory activity against human hepatocellular carcinoma cells (SMMC-7721) using MTT assay, and 5-Fluorouracil (5-FU) and adriamycin (ADM) were used as the positive compounds. As shown in Fig. 2, ADM significantly inhibited the proliferation of the cells. It was observed that most compounds strongly inhibited cell growth of these cancer cell lines at 25 μM, superior to 5-FU. Interestingly, compounds **10A-N** with an aryl group showed greater inhibition of cancer cells than compounds **10a-n** with an ethyl group at the R^1 positions, especially, **10A**, **10B**, **10E-J**, and **10L-N** comparable to ADM with the inhibition by 80%.

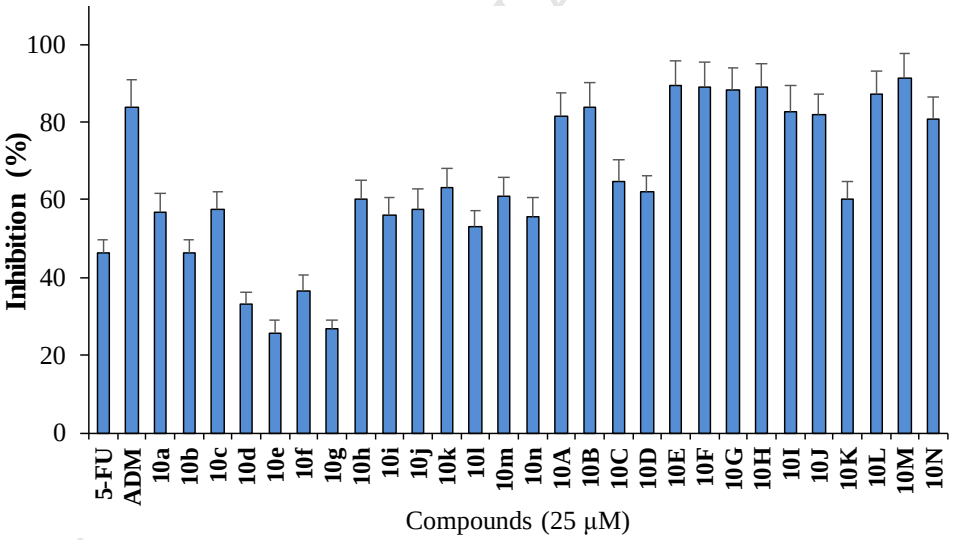

Fig. 2. Inhibition of cell proliferation (%) of target compounds against SMMC-7721 cell lines after incubation for 72 h at a concentration of 25 μM. Data are expressed as means + SD of each compound from three separate measurements.

These active compounds **10A**, **10B**, **10E-J**, and **10L-N** were further assayed for their antiproliferative activity against three cancer cell lines including hepatocellular carcinoma cells (SMMC-7721), human colonic carcinoma cells (HCT116), and human gastric cancer cells (SGC-7901) by MTT assay. IC_{50} values of the tested compounds against three tumor cell lines above were listed in Table 1. All tested compounds displayed antiproliferative potency in the low micromolar range in all three cells, which were much better than those of 5-FU. Especially, compounds **10E-G**, **10L**, and **10M** exhibited significant antiproliferative effects with the IC_{50} values of 0.76-5.84 μM, which were comparable to or better than ADM (IC_{50} = 2.31-4.12 μM). Notably, **10M** exhibited the most potent inhibitory activity with IC_{50} values of 0.76-2.01 μM against all tested cancer cells, which were nearly two- to three-fold better than ADM and seventeen- to fifty-fold more potent than 5-FU (IC_{50} = 29.5-37.8 μM).

Table 1. IC_{50} values of compounds **10A**, **10B**, **10E-J**, and **10L-N** against three human cancer cell lines[a]

Compd.	*In vitro* antiproliferative activity (IC_{50}[a], μM)		
	SMMC-7721	SGC7901	HCT116
10A	6.64 ± 0.72	7.08 ± 0.65	8.02 ± 0.67

10B	7.97 ± 0.91	8.11 ± 0.76	6.03 ± 0.55
10E	5.23 ± 0.48	4.62 ± 0.52	2.91 ± 0.37
10F	2.05 ± 0.33	2.84 ± 0.36	1.18 ± 0.23
10G	5.21 ± 0.65	2.97 ± 0.41	2.31 ± 0.26
10H	3.23 ± 0.29	4.43 ± 0.52	7.25 ± 0.66
10I	6.82 ± 0.77	7.51 ± 0.90	4.67 ± 0.49
10J	7.13 ± 0.68	5.96 ± 0.49	5.91 ± 0.65
10L	5.84 ± 0.65	3.73 ± 0.38	2.85 ± 0.33
10M	**0.76 ± 0.11**	**2.01 ± 0.31**	**1.26 ± 0.25**
10N	8.67 ± 0.56	3.22 ± 0.44	3.02 ± 0.29
5-Fluorouracil	37.8 ± 4.62	34.4 ± 4.15	29.5 ± 3.76
ADM	2.67 ± 0.25	4.12 ± 0.38	2.31 ± 0.30

[a] The inhibitory effects of individual compounds on the proliferation of cancer cell lines were determined by the MTT assay. The data are expressed as the mean ± SD of three independent experiments data.

Given the strong growth inhibitory activity of **10M** *in vitro*, the selectivity profile was investigated by examining its inhibitory effects on the growth of both cancer cells SMMC-7721 and normal liver cells LO2. It was found that treatment with increased dose of **10M** had no significant effect on the survival of non-tumor LO2 cells while the same treatment induced majority of SMMC-7721 cell death (Fig. 3), suggesting **10M** might possess selective antiproliferative activity against tumor cells.

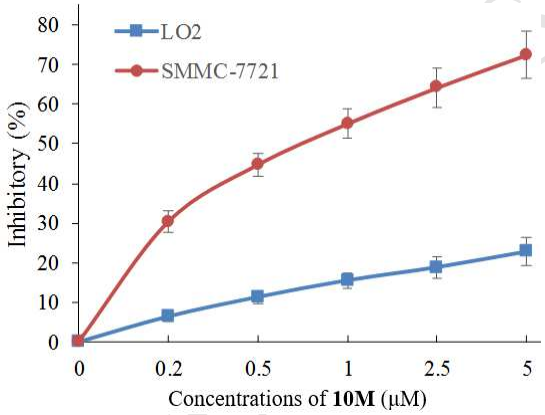

Fig. 3. Inhibitory effects of **10M** on the proliferation of SMMC-7721 and LO2 cells. Cells were incubated with the indicated concentrations of **10M** for 72 h. Cell proliferation was assessed using the MTT assay. Data are means ± SD of the inhibition (%) from three independent experiments.

The Structure–activity relationship (SAR) studies of designed compounds revealed that the R^1 and R^2 groups have significant impacts on inhibiting cell growth. As for R^1 substituent, compounds **10A-N** with an aryl ring displayed stronger anti-proliferative activity against tested cancer cells than the corresponding compounds **10a-n** carrying an ethyl moiety. As for R^2 group, compounds **10E-G** and **10L-N** containing methyl, methoxy, or trifluoromethoxy group indicated more potent activity than the corresponding compounds **10A-D** and **10H-K** containing halogen group.

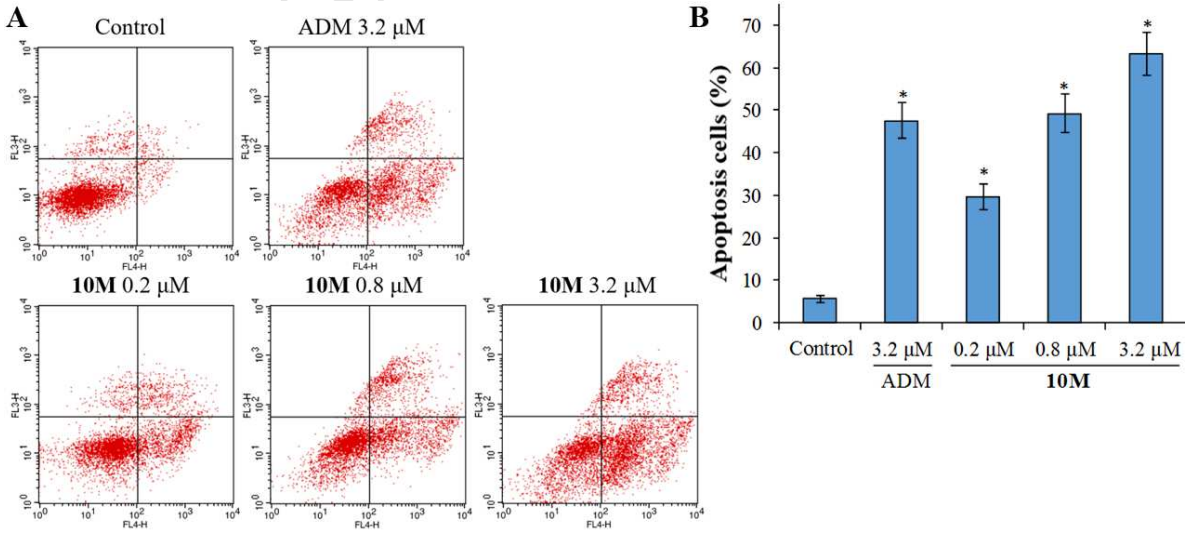

Fig. 4. Compound **10M** induces SMMC-7721 cell apoptosis *in vitro*. SMMC-7721 cells were incubated with the indicated concentrations of **10M**, or ADM (3.2 μM) for 72 h, and the cells were stained with FITC-Annexin V/PI, followed by flow cytometry analysis. (A) Flow cytometry analysis. (B) Quantitative analysis of apoptotic cells. Data are expressed as means ± SD of the percentages of apoptotic cells from three independent experiments. **P*< 0.01 vs control.

*2.3. Compound **10M** induces apoptosis in SMMC-7721 cells*

To determine whether the inhibitory effects of **10M** on hepatocellular carcinoma cell proliferation are accompanied by enhanced cancer cell apoptosis, SMMC-7721 cells were incubated with different concentrations of **10M**, or ADM for 72 h, and the percentages of apoptotic cells were determined by FITC-Annexin V/PI staining and flow cytometry. As shown in Fig. 4, the percentage of annexin V + apoptotic SMMC-7721 cells gradually increased for those cells exposed to the increasing concentrations of **10M** (29.6% for 0.2 μM; 49.2% for 0.8 μM; and 63.2% for 3.2 μM), which demonstrating that the incubation with **10M** induced SMMC-7721 cell apoptosis in a dose-dependent manner. In contrast, incubations performed using ADM (3.2 μM) only induced apoptosis of 47.5% SMMC-7721 cells.

To further investigate the apoptosis induction of **10M**, we examined the expression of apoptotic proteins Bax, Bcl-2, and the cleavage states of caspase-3 and PARP, in response to **10M** treatment (Fig. 5). Sub-confluent SMMC-7721 hepatocellular carcinoma cells were treated with or without **10M** for 72 h, and then lysed and analyzed by western blot. *β*-Actin expression was used as an internal control. It indicated that treatment with **10M** dramatically increased pro-apoptotic Bax expression in the relative levels, but reduced the anti-apoptotic Bcl-2 expression in a dose-dependent manner. Furthermore, compound **10M** resulted in more significant cleavage of both PARP and caspase-3 than the control group (Fig. 5). Importantly, **10M** treatment also induced more cleavage of PARP and caspase-3 than the AMD treated group at the same concentration of 3.2 μM. Taken together, these results confirmed that **10M** treatment induced apoptosis in SMMC-7721 cells.

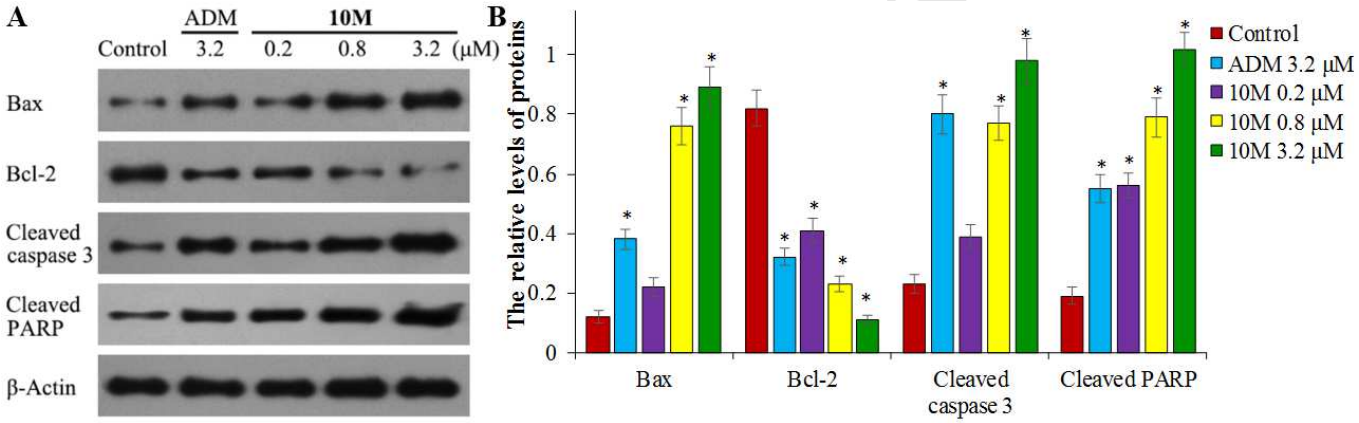

Fig. 5. (A) The expression of Bax, Bcl-2, cleaved Caspase 3 and PARP, and *β*-actin was examined by western blot analysis. SMMC-7721 cells were incubated with, or without, **10M** and ADM at the indicated concentrations for 72 h and the levels of protein expression were detected using specific antibodies. Data shown are representative images of each protein for three separate experiments. (B) Quantitative analysis of Bax, Bcl-2, and cleaved Caspase 3 and PARP. The relative levels of each protein compared to control *β*-actin were determined by densimetric scanning. Data are expressed as means ± SD from three separate experiments. **P* < 0.01 vs respective control.

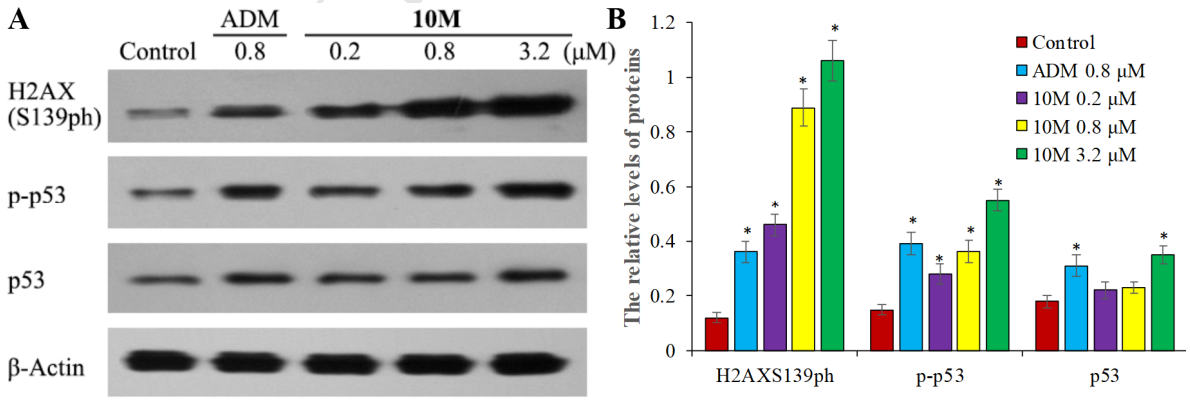

Fig. 6. Immunoblot analysis of the expression of DNA damage and DNA-damage response p53 activation *in vitro*. (A) SMMC-7721 cells were treated with vehicle (control), different doses of **10M**, or ADM were homogenized, and their lysates were subjected to immunoblot analysis using anti-H2AXS139ph, antiphospho-p53 (ser15), anti-p53, and anti-*β*-actin antibodies, respectively. *β*-Actin was used as the control. (B) Quantitative analysis. The relative levels of each signaling event to control *β*-actin were determined by densimetric scanning. The data are expressed as means ± SD from three separate experiments. **P* < 0.01 vs respective control.

*2.4. Compound **10M** induces DNA damage and activates the p53 signaling pathway*

It is well-known that DNA damage is one of the molecular events associated with cell apoptosis [39]. Histone H2A.X, a variant form of histone H2A, is required for checkpoint-mediated DNA repair following double-stranded DNA breaks [40]. To verify whether the anti-cancer activities of bis-pyrazole derivatives were partly from DNA damage, we examined the DNA damage extent and the change of the DNA-damage response p53 signaling pathway caused by **10M** in HCC cells. In the present study, we used histone H2AX phosphorylation as DNA damage markers. SMMC-7721 cells were treated with vehicle or **10M** for 72 h, using ADM as positive controls. H2AXS139ph and p-p53 (ser15) were then detected using western blot analysis. As shown in Fig. 6, treatment with **10M** dose-dependently increased the levels of H2AX phosphorylation in SMMC-7721 cells. Importantly, H2AXS139ph level in both 0.8 μM and 3.2 μM **10M** treatment groups was significantly higher than that in 0.8 μM ADM group.

p53 is an important tumor suppressor protein that plays a major role in cellular response to DNA damage. Ser 15, a common site for a variety of kinases such as ATM/ATR/DNA-NK, is activated during the DNA repair pathway. p53 acts as a nuclear transcription factor and transactivates multiple genes involved in apoptosis progress [41]. To evaluate the effect of new compounds on p53 activation, SMMC-7721 cells were cultured in the presence of **10M** for 72 h at 0.2, 0.8, and 3.2 μM concentrations, respectively. Western blotting results showed a significantly increased p53 phosphorylation at Ser15 in response to **10M** treatment in dose-dependent manner (Fig. 6). These results demonstrated that the activation of p53 as downstream signaling molecules in response to DNA damage induced by new bis-pyrazole derivatives.

*2.5. In vivo anti-cancer activity of **10M***

To evaluate the safety of **10M** *in vivo*, groups of ICR mice were injected intraperitoneally with a single dose of **10M** or vehicle control, respectively. The survival of mice was monitored up to 14 days after injection. Only one mice that had been treated with **10M** at the highest dose (488.3 mg/kg) survived (shown in Table 2). In contrast, injection with **10M** at the lowest dose (200 mg/kg) did not cause any death and abnormality in eating, drinking, body weight, and activity throughout the observation period. As a result, the LD_{50} value of **10M** was calculated to be 349.6 mg/kg for this train of mice.

Next, we established a BALB/c nude mice model which was inoculated subcutaneously with SMMC-7721 cells to evaluate the *in vivo* antitumor activity of **10M**. After the establishment of solid tumor, BALB/c nude mice were randomly intraperitoneally administered with **10M**, ADM, and vehicle, respectively. The changes in tumor volumes and weights were measured over 19 days. Compared with the vehicle control, treatment with **10M** significantly reduced the tumor volume growth rate in a dose-dependent manner (Fig. 7). It was observed that treatment with **10M** (30 mg/kg) strongly inhibited the growth of the tumor cells *in vivo* similar to ADM at the dose of 15 mg/kg. Importantly, the tumor weights (0.61 ± 0.04, 0.38 ± 0.02 g) in the mice treated with **10M** at 15 and 30 mg/kg, respectively, were significantly reduced by 44.00% and 65.35% compared to the vehicle-treated controls (1.09 ± 0.02 g, $p < 0.01$). Besides, there was no statistical difference in body weight in postinoculation among the four groups of mice. Together, our data clearly demonstrated that **10M** could evidently inhibit the growth of tumor *in vivo*.

Table 2 The acute toxicity of **10M** in mice

Dose (mg/kg)	Number of mice	Number of dead mice							Total death	Survival (%) on day 14
		1h	4h	1d	2d	3d	4d	5-14d		
488.3	10	0	0	1	1	2	2	3	9	10
390.6	10	0	0	1	1	2	1	1	6	40
312.5	10	0	0	1	1	0	2	0	4	60
250.0	10	0	0	1	1	1	0	0	3	70
200.0	10	0	0	0	0	0	0	0	0	100

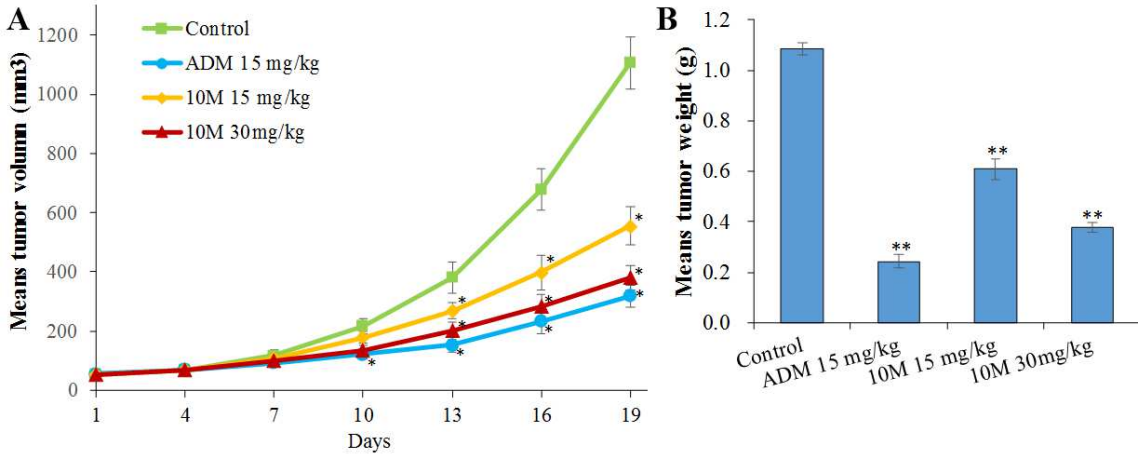

Fig. 7. Inhibitory effects of **10M** on the growth of an implanted SMMC-7721 xenograft in nude mice. BALB/c nude mice were subcutaneously inoculated with SMMC-7721 cells. After establishment of solid tumor, the mice were randomized and treated with solvent control, ADM, or **10M** at the indicated doses, respectively. The growth of tumors was measured longitudinally. Data are expressed as means (SD of tumor volumes at each time point for each group of mice (n = 6 per group)). *$P < 0.01$ vs control group.

3. Conclusions

In summary, we designed and synthesized a series of new bis-pyrazole compounds and investigated their antitumor effects *in vitro* and *in vivo*. Some compounds displayed potent cell growth inhibitory activity with IC_{50} values in low-micromolar range against three human cancer cells *in vitro*. The most potent compound **10M** possessed stronger antiproliferative activity of cancer cells than ADM, and did not affect proliferation of non-tumor LO2 cells in the effective dose against cancer cells. In addition, **10M** exhibited a significant induction of cell apoptosis through marked cleavage of both PARP and caspase-3. Furthermore, our study demonstrated that the potent activity in the cell growth inhibition and apoptosis induction effects of **10M** may be related to DNA damage and activation of the p53 signaling pathway. Finally, **10M** displayed low acute toxicity and significant growth inhibition of cancer cells *in vivo*.

4. Experimental section

4.1. General methods and materials

^{1}H NMR and ^{13}C NMR spectra were obtained on a Bruker AV400 spectrometer (Bruker Co., Switzerland) in $CDCl_3$ solution with tetramethylsilane as the internal standard. Chemical shift values (δ) are given in parts per million. The melting points were determined on an X-4 binocular microscope melting point apparatus (Beijing Tech Instrument Co., Beijing, China) and are uncorrected. High resolution mass spectra (HRMS) were recorded on Shimadzu LCMS-IT-TOF. Compounds **1a-c**, **2a-c**, and **7-9** were synthesized according the methods of literatures [36-38]. The reagents used were of analytical grade, where the anhydrous reagents were used after pretreatment. All anhydrous solvents were dried and purified by standard techniques.

*4.1.1. General procedure for the preparation of compounds **3a-c***

To a solution of compound **2** (77 mmol) in dichloromethane (100 mL) was added sodium carbonate (107 mmol), the resulting mixture was heated to 40 □. To the above solution was added dimethyl sulfate (107 mmol). The mixture was refluxed for 24 h, and then the reaction mixture was poured in water and extracted with dichloromethane. The combined extracts were dried over anhydrous sodium sulfate and filtered, the crude product was concentrated and was purified by silica gel column chromatography (hexane-EtOAc, 20:1 elution) to give compounds **3a-c**.

*Ethyl 3-ethyl-1-methyl-1H-pyrazole-5-carboxylate (**3a**)*. Yellow oil; yield, 75%; ^{1}H NMR (400 MHz, $CDCl_3$) δ: 6.64 (s, 1H, Pyrazole-H), 4.34 (q, J=7.2 Hz, 2H, OCH_2), 4.12 (s, 3H, N-CH_3), 2.64 (q, J=7.6 Hz, 2H, CH_2), 1.37 (t, J=7.2 Hz, 3H, CH_3), 1.24 (t, J=7.6 Hz, 3H, CH_3). ^{13}C NMR (100 MHz, $CDCl_3$) δ: 160.0, 153.1, 132.9, 108.9, 60.9, 39.1, 21.2, 14.3, 13.8.

*Ethyl 3-(4-fluorophenyl)-1-methyl-1H-pyrazole-5-carboxylate (**3b**)*. White solid; yield, 68%; mp: 72-74 °C; ^{1}H NMR (400 MHz, $CDCl_3$) δ: 7.73 (d, J=6.8 Hz, 2H, Ar-H), 7.37 (d, J=8.4 Hz, 2H, Ar-H), 7.09 (s, 1H, Pyrazole-H), 4.38 (q, J=7.2 Hz, 2H, OCH_2), 4.12 (s, 3H, N-CH_3), 1.40 (t, J=7.2 Hz, 3H, CH_3). ^{13}C NMR (100 MHz, $CDCl_3$) δ: 159.7, 148.6, 133.9, 133.8, 131.1, 128.9, 126.7, 107.8, 61.2, 39.7, 14.3.

*Ethyl 3-(4-chlorophenyl)-1-methyl-1H-pyrazole-5-carboxylate (**3c**)*. White solid; yield, 71%; mp: 77-79 °C; ^{1}H NMR (400 MHz, $CDCl_3$) δ: 7.73 (d, J=8.4 Hz, 2H, Ar-H), 7.37 (d, J=8.4 Hz, 2H, Ar-H), 7.10 (s, 1H, Pyrazole-H), 4.39 (q, J=7.2 Hz, 2H, OCH_2), 4.23 (s, 3H, N-CH_3), 1.41 (t, J=7.2 Hz, 3H, CH_3). ^{13}C NMR (100 MHz, $CDCl_3$) δ: 159.7, 148.6, 134.0, 133.9, 130.9, 128.9, 126.8, 107.8, 61.2, 39.7, 14.3.

*4.1.2. General procedure for the preparation of compounds **4a-c***

To a solution of compound **3** (40 mmol) in 1,2-dichloroethane (100 mL) was added dropwise sulfuryl chloride (44 mmol). The reaction mixture was refluxed for 4 h. After the completion of reaction, the mixture was added water (100 mL), the product was extracted from water with ethyl acetate. The combined extracts were dried over anhydrous sodium sulfate, filtered, and evaporated to produce compounds **4a-c**.

*Ethyl 4-chloro-3-ethyl-1-methyl-1H-pyrazole-5-carboxylate (**4a**)*. Yellow oil; yield, 83%; ^{1}H NMR (400 MHz, $CDCl_3$) δ: 4.41 (q, J=7.2 Hz, 2H, CH_2), 4.09 (s, 3H, N-CH_3), 2.66 (q, J=7.6 Hz, 2H, CH_2), 1.41 (t, J=7.2 Hz, 3H, CH_3), 1.24 (t, J=7.6 Hz, 3H, CH_3). ^{13}C NMR (100 MHz, $CDCl_3$) δ: 159.2, 150.4, 129.1, 113.1, 61.3, 40.6, 19.2, 14.2, 12.8.

*Ethyl 4-chloro-3-(4-fluorophenyl)-1-methyl-1H-pyrazole-5-carboxylate (**4b**)*. White solid; yield, 75%; mp: 83-85 °C; ^{1}H NMR (400 MHz, $CDCl_3$) δ: 7.83 (d, J=8.4 Hz, 2H, Ar-H), 7.41 (d, J=8.8 Hz, 2H, Ar-H), 4.45 (q, J=7.2 Hz, 2H, CH_2), 4.19 (s, 3H, N-CH_3), 1.44 (t, J=7.2 Hz, 3H, CH_3). ^{13}C NMR (100 MHz, $CDCl_3$) δ: 159.0, 145.7, 134.4, 130.4, 129.5, 128.9, 128.7, 112.5, 61.6, 41.2, 14.2.

*Ethyl 4-chloro-3-(4-fluorophenyl)-1-methyl-1H-pyrazole-5-carboxylate (**4c**)*. White solid; yield, 78%; mp: 76-78 °C; ^{1}H NMR (400 MHz, $CDCl_3$) δ: 7.82 (d, J=8.4 Hz, 2H, Ar-H), 7.41 (d, J=8.4 Hz, 2H, Ar-H), 4.45 (q, J=7.2 Hz, 2H, CH_2), 4.18 (s, 3H, N-CH_3), 1.44 (t, J=7.2 Hz, 3H, CH_3). ^{13}C NMR (100 MHz, $CDCl_3$) δ: 159.0, 145.7, 134.4, 130.4, 129.5, 128.7, 112.5, 61.6, 41.2, 14.2.

*4.1.3. General procedure for the preparation of compounds **5a-c***

To a cold solution of compound **4** (40 mmol) in THF (100 mL) was added $LiAlH_4$ (80 mmol) in portions. After addition, the reaction mixture was stirred at room temperature for 1 h. After completion of the reaction, the mixture was cooled by ice-water bath as added water slowly. Then the mixture was filtered, the filtrate was extracted with ethyl acetate. The combined extracts were dried over anhydrous sodium sulfate, filtered and evaporated to afford compounds **5a-c**.

*(4-Chloro-3-ethyl-1-methyl-1H-pyrazol-5-yl)methanol (**5a**)*. White solid; yield, 69%; mp: 125-127 °C; ^{1}H NMR (400 MHz, $CDCl_3$) δ: 4.62 (s, 2H, CH_2), 3.83 (s, 3H, N-CH_3), 2.59 (q, J=7.6 Hz, 2H, CH_2), 1.21 (t, J=7.6 Hz, 3H, CH_3). ^{13}C NMR (100 MHz, $CDCl_3$) δ: 149.5, 137.7, 107.4, 53.0, 37.1, 19.4, 13.0.

*[4-Chloro-3-(4-fluorophenyl)-1-methyl-1H-pyrazol-5-yl]methanol (**5b**).* White solid; yield, 63%; mp: 112-114 °C; ^{1}H NMR (400 MHz, $CDCl_3$) δ: 7.82 (d, *J*=8.8 Hz, 2H, Ar-H), 7.39 (d, *J*=8.4 Hz, 2H, Ar-H), 4.72 (s, 2H, CH_2), 3.96 (s, 3H, N-CH_3). ^{13}C NMR (100 MHz, $CDCl_3$) δ: 144.7, 139.0, 134.0, 130.1, 129.0, 128.7, 128.4, 115.5, 107.1, 53.2, 37.7.

*[4-Chloro-3-(4-chlorophenyl)-1-methyl-1H-pyrazol-5-yl]methanol (**5c**).* White oil; yield, 65%; ^{1}H NMR (400 MHz, $CDCl_3$) δ: 7.81 (d, *J*=8.8 Hz, 2H, Ar-H), 7.39 (d, *J*=8.8 Hz, 2H, Ar-H), 4.71 (s, 2H, CH_2), 3.95 (s, 3H, N-CH_3). ^{13}C NMR (100 MHz, $CDCl_3$) δ: 144.7, 139.0, 134.0, 130.1, 128.7, 128.4, 107.0, 53.2, 37.7.

*4.1.4. General procedure for the preparation of compounds **6a-c***

To a cold solution of compound **5** (35 mmol) in dichloromethane (100 mL) was added dropwise thionyl chloride (70 mmol). The resulting mixture was stirred at room temperature for another 1 h. The mixture was cooled by ice-water bath and water was slowly added thereto. The product was extracted with ethyl acetate. The combined extracts were dried over anhydrous sodium sulfate, filtered and evaporated to obtain compounds **6a-c**.

*4-Chloro-5-(chloromethyl)-3-ethyl-1-methyl-1H-pyrazole (**6a**).* White solid; yield, 62%; mp: 67-69 °C; ^{1}H NMR (400 MHz, $CDCl_3$) δ: 4.58 (s, 2H, CH_2), 3.87 (s, 3H, N-CH_3), 2.63 (q, *J*=7.6 Hz, 2H, CH_2), 1.24 (t, *J*=7.6 Hz, 3H, CH_3). ^{13}C NMR (100 MHz, $CDCl_3$) δ: 149.7, 134.5, 108.6, 37.2, 32.6, 19.4, 12.8.

*4-Chloro-5-(chloromethyl)-3-(4-fluorophenyl)-1-methyl-1H-pyrazole (**6b**).* White solid; yield, 58%; mp: 56-58 °C; ^{1}H NMR (400 MHz, $CDCl_3$) δ: 7.83 (d, *J*=8.4 Hz, 2H, Ar-H), 7.39 (d, *J*=8.8 Hz, 2H, Ar-H), 4.65 (s, 2H, CH_2), 3.97 (s, 3H, N-CH_3). ^{13}C NMR (100 MHz, $CDCl_3$) δ: 164.0, 145.0, 136.0, 134.2, 129.9, 129.0, 128.7, 115.6, 108.1, 37.7, 32.5.

*4-Chloro-5-(chloromethyl)-3-(4-chlorophenyl)-1-methyl-1H-pyrazole (**6c**).* White oil; yield, 55%; ^{1}H NMR (400 MHz, $CDCl_3$) δ: 7.83 (d, *J*=8.4 Hz, 2H, Ar-H), 7.39 (d, *J*=8.4 Hz, 2H, Ar-H), 4.65 (s, 2H, CH_2), 3.97 (s, 3H, N-CH_3). ^{13}C NMR (100 MHz, $CDCl_3$) δ: 145.0, 136.0, 134.2, 129.9, 128.7, 128.3, 108.1, 37.7, 32.5.

*4.1.5. General procedure for the preparation of the target compounds **10a-n** and **10A-N***

To a solution of compound **6** (12 mmol) and compound **9** (10 mmol) in acetonitrile (40 mL) was added potassium carbonate (20 mmol) and cesium carbonate (5 mmol). The resulting reaction mixture was refluxed for 12-18 h. On completion of the reaction, the mixture was filtered and the solution was evaporated to give the crude product, which was recrystallized from a mixture of ethyl acetate and petroleum ether to afford the title compounds **10a-n** and **10A-N**.

*5-(4-Fluorophenoxy)-1-methyl-3-methyl-1H-pyrazole-4-carbaldehyde-O-[(4-chloro-3-ethyl-1-methyl-1H-pyrazol-5-yl)methyl]oxime (**10a**).* White solid; yield, 79%; mp: 72-74 °C; ^{1}H NMR (400 MHz, $CDCl_3$) δ: 7.74 (s, 1H, CH=N), 7.00 (t, *J* = 8.6 Hz, 2H, Ar-H), 6.86-6.83 (m, 2H, Ar-H), 4.97 (s, 2H, CH_2), 3.78 (s, 3H, N-CH_3), 3.59 (s, 3H, N-CH_3), 2.61 (q, *J* = 7.6 Hz, 2H, CH_2), 2.35 (s, 3H, CH_3), 1.22 (t, *J* = 7.6Hz, 3H, CH_3). ^{13}C NMR (100 MHz, $CDCl_3$) δ: 158.8, 152.6, 149.4, 147.9, 147.1, 141.3, 135.2, 116.7, 116.6, 116.5, 109.1, 99.7, 63.8, 37.3, 34.3, 19.4, 14.8, 13.0. HRMS (ESI) m/z calcd for $C_{19}H_{22}ClFN_5O_2$, 406.1446; found, 406.1441 $[M + H]^+$.

*5-(2-Fluorophenoxy)-1-methyl-3-methyl-1H-pyrazole-4-carbaldehyde-O-[(4-chloro-3-ethyl-1-methyl-1H-pyrazol-5-yl)methyl]oxime (**10b**).* White solid; yield, 78%; mp: 58-60 °C; ^{1}H NMR (400 MHz, $CDCl_3$) δ: 7.75 (s, 1H, CH=N), 7.19 (m, 1H, Ar-H), 7.06 (m, 2H, Ar-H), 6.76 (m , 1H, Ar-H). 4.95 (s, 2H, CH_2), 3.77 (s, 3H, N-CH_3), 3.64 (s, 3H, N-CH_3), 2.60 (q, *J* = 7.6 Hz, 2H, CH_2), 2.34 (s, 3H, CH_3), 1.22 (t, *J* = 7.6 Hz, 3H, CH_3). ^{13}C NMR (100 MHz, $CDCl_3$) δ: 151.9, 149.4, 147.5, 147.0, 141.1, 135.2, 124.7, 124.6, 124.5, 117.3, 117.1, 116.6, 109.1, 99.6, 63.3, 37.4, 34.3, 19.4, 14.6, 13.0. HRMS (ESI) m/z calcd for $C_{19}H_{22}ClFN_5O_2$, 406.1446; found, 406.1443 $[M + H]^+$.

*5-(4-Chlorophenoxy)-1-methyl-3-methyl-1H-pyrazole-4-carbaldehyde-O-[(4-chloro-3-ethyl-1-methyl-1H-pyrazol-5-yl)methyl]oxime (**10c**).* White solid; yield, 80%; mp: 74-75 °C; ^{1}H NMR (400 MHz, $CDCl_3$) δ: 7.75 (s, 1H, CH=N), 7.28 (d, *J* = 9.2 Hz, 2H, Ar-H), 6.83 (d, *J* = 8.8 Hz, 2H, Ar-H), 4.95 (s, 2H, CH_2), 3.77 (s, 3H, N-CH_3), 3.64 (s, 3H, N-CH_3), 2.60 (q, *J* = 7.6 Hz, 2H, CH_2), 2.34 (s, 3H, CH_3), 1.22 (t, *J* = 7.6 Hz, 3H, CH_3). ^{13}C NMR (100 MHz, $CDCl_3$) δ: 155.1, 149.4, 147.4, 147.1, 141.2, 135.2, 130.0, 128.9, 116.6, 109.1, 99.9, 63.4, 37.4, 34.3, 19.4, 14.7, 13.0. HRMS (ESI) m/z calcd for $C_{19}H_{22}Cl_2N_5O_2$, 422.1151; found, 422.1141 $[M + H]^+$.

*5-(3-Chlorophenoxy)-1-methyl-3-methyl-1H-pyrazole-4-carbaldehyde-O-[(4-chloro-3-ethyl-1-methyl-1H-pyrazol-5-yl)methyl]oxime (**10d**).* White solid; yield, 78%; mp: 77-78 °C; ^{1}H NMR (400 MHz, $CDCl_3$) δ: 7.76 (s, 1H, CH=N), 7.25 (t, *J* = 8.0 Hz, 1H, Ar-H), 7.10 (d, *J* = 8.0 Hz, 1H, Ar-H), 6.90 (s, 1H, Ar-H), 6.79-6.76 (m, 1H, Ar-H), 4.97 (s, 2H, CH_2), 3.78 (s, 3H, N-CH_3), 3.58 (s, 3H, N-CH_3), 2.60 (q, *J* = 7.6 Hz, 2H, CH_2), 2.36 (s, 3H, CH_3), 1.22 (t, *J* = 7.6 Hz, 3H, CH_3). ^{13}C NMR (100 MHz, $CDCl_3$) δ: 157.1, 149.4, 147.1, 147.0, 141.2, 135.52, 135.2, 130.8, 124.1, 115.9, 113.5, 109.1, 100.0, 63.4, 37.4, 34.3, 19.4, 14.7, 13.0. HRMS (ESI) m/z calcd for $C_{19}H_{22}Cl_2N_5O_2$, 422.1151; found, 422.1141 $[M + H]^+$.

*5-(2-Chlorophenoxy)-1-methyl-3-methyl-1H-pyrazole-4-carbaldehyde-O-[(4-chloro-3-ethyl-1-methyl-1H-pyrazol-5-yl)methyl]oxime (**10e**).* White solid; yield, 79%; mp: 73-75 °C; ^{1}H NMR(400 MHz, $CDCl_3$) δ: 7.74 (s, 1H, CH=N), 7.45 (m, 1H, Ar-H), 7.16 (m, 1H, Ar-H), 7.07 (m, 1H, Ar-H), 6.68 (m, 1H, Ar-H), 4.95 (s, 2H, CH_2), 3.77 (s, 3H, N-CH_3), 3.62 (s, 3H, N-CH_3), 2.60 (q, *J* = 7.6 Hz, 2H, CH_2), 2.35 (s, 3H, CH_3), 1.22 (t, *J* = 7.6 Hz, 3H, CH_3). ^{13}C NMR (100 MHz, $CDCl_3$) δ: 152.1, 149.4, 147.3, 147.1, 141.1, 135.1, 131.0, 128.1, 124.7, 122.7, 115.5, 109.0, 99.9, 63.4, 37.4, 34.3, 19.4, 14.7, 13.0. HRMS (ESI) m/z calcd for $C_{19}H_{22}Cl_2N_5O_2$, 422.1151; found, 422.1149 $[M + H]^+$.

*5-(4-Bromophenoxy)-1-methyl-3-methyl-1H-pyrazole-4-carbaldehyde-O-[(4-chloro-3-ethyl-1-methyl-1H-pyrazol-5-yl)methyl]oxime (**10f**).*White solid; yield, 77%; mp: 79-81 °C; ^{1}H NMR (400 MHz, $CDCl_3$) δ: 7.75 (s, 1H, CH=N), 7.42 (d, *J* = 8.8 Hz, 2H, Ar-H), 6.78 (d, *J* = 9.2 Hz, 2H, Ar-H), 4.96 (s, 2H, CH_2), 3.78 (s, 3H, N-CH_3), 3.59 (s, 3H, N-CH_3), 2.61 (q, *J* = 7.6 Hz, 2H, CH_2), 2.35 (s, 3H, CH_3), 1.22 (t, *J* = 7.6 Hz, 3H, CH_3). ^{13}C NMR (100 MHz, $CDCl_3$) δ: 155.7, 149.4, 147.3, 147.1, 141.2, 135.2, 132.9, 117.0, 116.3, 109.1, 99.9, 63.3, 37.4, 34.3, 19.4, 14.7, 13.0. HRMS (ESI) m/z calcd for $C_{19}H_{22}BrClN_5O_2$, 466.0645; found, 466.0635 $[M + H]^+$.

5-(4-Iodophenoxy)-1-methyl-3-methyl-1H-pyrazole-4-carbaldehyde-O-[(4-chloro-3-ethyl-1-methyl-1H-pyrazol-5-yl)methyl]oxime ***(10g)***. White solid; yield, 78%; mp: 127-129 °C; ^{1}H NMR (400 MHz, $CDCl_3$) δ: 7.74 (s, 1H, CH=N), 7.61 (d, J = 8.8 Hz, 2H, Ar-H), 6.66 (d, J = 8.8 Hz, 2H, Ar-H), 4.96 (s, 2H, CH_2), 3.78 (s, 3H, N-CH_3), 3.58 (s, 3H, N-CH_3), 2.61 (q, J = 7.6 Hz, 2H, CH_2), 2.34 (s, 3H, CH_3), 1.22 (t, J = 7.6 Hz, 3H, CH_3). ^{13}C NMR (100 MHz, $CDCl_3$) δ: 156.5, 149.4, 147.2, 147.1, 141.2, 138.9, 135.2, 117.5, 109.1, 99.9, 86.6, 63.4, 37.4, 34.3, 19.4, 14.7, 13.0. HRMS (ESI) m/z calcd for $C_{23}H_{21}ICIFN_5O_2$, 514.0507; found, 514.0497 $[M + H]^+$.

5-(4-Methylphenoxy)-1-methyl-3-methyl-1H-pyrazole-4-carbaldehyde-O-[(4-chloro-3-ethyl-1-methyl-1H-pyrazol-5-yl)methyl]oxime ***(10h)***. White solid; yield, 77%; mp: 52-53 °C; ^{1}H NMR (400 MHz, $CDCl_3$) δ: 7.75 (s, 1H, CH=N), 7.10 (d, J = 8.4 Hz, 2H, Ar-H), 6.77 (d, J = 8.4 Hz, 2H, Ar-H), 4.96 (s, 2H, CH_2), 3.78 (s, 3H, N-CH_3), 3.58 (s, 3H, N-CH_3), 2.60 (q, J = 7.6 Hz, 2H, CH_2), 2.35 (s, 3H, CH_3), 2.31 (s, 3H, CH_3), 1.22 (t, J = 7.6 Hz, 3H, CH_3). ^{13}C NMR (100 MHz, $CDCl_3$) δ: 154.6, 149.4, 148.3, 146.9, 141.6, 135.3, 133.3, 130.4, 115.1, 109.0, 99.8, 63.3, 37.4, 34.2, 20.6, 19.4, 15.0, 13.0. HRMS (ESI) m/z calcd for $C_{20}H_{25}ClN_5O_2$, 402.1697; found, 402.1693 $[M + H]^+$.

5-(3-Methylphenoxy)-1-methyl-3-methyl-1H-pyrazole-4-carbaldehyde-O-[(4-chloro-3-ethyl-1-methyl-1H-pyrazol-5-yl)methyl]oxime ***(10i)***. Yellow solid; yield, 79%; mp: 75-76 °C; ^{1}H NMR(400 MHz, $CDCl_3$) δ: 7.76 (s, 1H, CH=N), 7.18 (t, J = 7.8 Hz, 1H, Ar-H), 6.91 (d, J = 7.2 Hz, 1H, Ar-H), 6.67 (d, J = 8.4 Hz, 2H, Ar-H), 4.98 (s, 2H, CH_2), 3.78 (s, 3H, N-CH_3), 3.58 (s, 3H, N-CH_3), 2.61 (q, J = 7.6 Hz, 2H, CH_2), 2.37 (s, 3H, CH_3), 2.32 (s, 3H, CH_3), 1.22 (t, J = 7.6 Hz, 3H, CH_3). ^{13}C NMR (100 MHz, $CDCl_3$) δ: 156.7, 149.4, 148.1, 146.9, 141.6, 140.4, 135.3, 129.7, 124.5, 1115.8, 112.2, 109.0, 99.9, 63.3, 37.4, 34.3, 21.4, 19.4, 15.0, 13.0. HRMS (ESI) m/z calcd for $C_{20}H_{25}ClN_5O_2$, 402.1697; found, 402.1693 $[M + H]^+$.

5-(2-Methylphenoxy)-1-methyl-3-methyl-1H-pyrazole-4-carbaldehyde-O-[(4-chloro-3-ethyl-1-methyl-1H-pyrazol-5-yl)methyl]oxime ***(10j)***. White solid; yield, 78%; mp: 92-94 °C; ^{1}H NMR (400 MHz, $CDCl_3$) δ: 7.69 (s, 1H, CH=N), 7.21 (d, J = 7.2 Hz, 1H, Ar-H), 7.10-6.99 (m, 2H, Ar-H), 6.52 (d, J = 8.0 Hz, 1H, Ar-H), 4.96 (s, 2H, CH_2), 3.76 (s, 3H, N-CH_3), 3.58 (s, 3H, N-CH_3), 2.60 (q, J = 7.6 Hz, 2H, CH_2), 2.38 (s, 3H, CH_3), 2.36 (s, 3H, CH_3), 1.22 (t, J = 7.6 Hz, 3H, CH_3). ^{13}C NMR (100 MHz, $CDCl_3$) δ: 154.9, 149.4, 148.4, 146.9, 141.6, 135.2, 131.6, 127.3, 126.5, 123.7, 113.4, 109.0, 99.6, 63.3, 37.4, 34.1, 19.4, 16.0, 14.9, 13.0. HRMS (ESI) m/z calcd for $C_{20}H_{25}ClN_5O_2$, 402.1697; found, 402.1695 $[M + H]^+$.

5-(4-Methoxyphenoxy)-1-methyl-3-methyl-1H-pyrazole-4-carbaldehyde-O-[(4-chloro-3-ethyl-1-methyl-1H-pyrazol-5-yl)methyl] oxime ***(10k)***. White solid; yield, 76%; mp: 56-58 °C; ^{1}H NMR (400 MHz, $CDCl_3$) δ: 7.73 (s, 1H, CH=N), 6.82 (s, 4H, Ar-H), 4.98 (s, 2H, CH_2), 3.79 (s, 3H, OCH_3), 3.78 (s, 3H, N-CH_3), 3.59 (s, 3H, N-CH_3), 2.61 (q, J = 7.6 Hz, 2H, CH_2), 2.35 (s, 3H, CH_3), 1.22 (t, J = 7.4 Hz, 3H, CH_3). ^{13}C NMR (100 MHz, $CDCl_3$) δ: 155.8, 150.6, 149.4, 148.7, 146.9, 141.6, 135.3, 116.3, 114.9, 109.1, 99.5, 63.3, 55.7, 37.4, 34.2, 19.4, 15.0, 13.0. HRMS (ESI) m/z calcd for $C_{20}H_{25}ClN_5O_3$, 418.1646; found, 418.1642 $[M + H]^+$.

5-(2-Methoxyphenoxy)-1-methyl-3-methyl-1H-pyrazole-4-carbaldehyde-O-[(4-chloro-3-ethyl-1-methyl-1H-pyrazol-5-yl)methyl] oxime ***(10l)***. White solid; yield, 78%; mp: 85-87 °C; ^{1}H NMR (400 MHz, $CDCl_3$) δ: 7.71 (s, 1H, CH=N), 7.11-7.07 (m, 1H, Ar-H), 6.98 (d, J = 7.2 Hz, 1H, Ar-H), 6.86-6.82 (m, 1H, Ar-H), 6.68 (d, J = 8.0 Hz, 1H, Ar-H), 4.96 (s, 2H, CH_2), 3.90 (s, 3H, OCH_3), 3.78 (s, 3H, N-CH_3), 3.61 (s, 3H, N-CH_3), 2.60 (q, J = 7.6 Hz, 2H, CH_2), 2.34 (s, 3H, CH_3), 1.22 (t, J = 7.6 Hz, 3H, CH_3). ^{13}C NMR (100 MHz, $CDCl_3$) δ: 149.3, 139.0, 146.7, 145.5, 141.5, 135.3, 124.9, 121.0, 116.0, 112.7, 108.9, 99.3, 63.3, 56.0, 37.4, 34.2, 19.4, 14.9, 13.0. HRMS (ESI) m/z calcd for $C_{20}H_{25}ClN_5O_3$, 418.1646; found, 418.1641 $[M + H]^+$.

5-(4-Trifluoromethoxyphenoxy)-1-methyl-3-methyl-1H-pyrazole-4-carbaldehyde-O-[(4-chloro-3-ethyl-1-methyl-1H-pyrazol-5-yl)methyl]oxime ***(10m)***. Yellow solid; yield, 75%; mp: 49-51 °C; ^{1}H NMR(400 MHz, $CDCl_3$) δ: 7.76 (s, 1H, CH=N), 7.18 (d, J = 8.8 Hz, 2H, Ar-H), 6.90 (d, J = 9.2 Hz, 2H, Ar-H), 4.95 (s, 2H, CH_2), 3.78 (s, 3H, N-CH_3), 3.60 (s, 3H, N-CH_3), 2.60 (q, J = 7.6 Hz, 2H, CH_2), 2.35 (s, 3H, CH_3), 1.22 (t, J = 7.6 Hz, 3H, CH_3). ^{13}C NMR (100 MHz, $CDCl_3$) δ: 154.9, 149.4, 147.3, 147.1, 144.8, 141.2, 135.2, 122.9, 120.4, 116.3, 109.1, 99.9, 63.3, 37.3, 34.3, 19.4, 14.7, 13.0. HRMS (ESI) m/z calcd for $C_{20}H_{22}ClF_3N_5O_3$, 472.1363; found, 472.1356 $[M + H]^+$.

5-(2-Trifluoromethoxyphenoxy)-1-methyl-3-methyl-1H-pyrazole-4-carbaldehyde-O-[(4-chloro-3-ethyl-1-methyl-1H-pyrazol-5-yl)methyl] oxime ***(10n)***. Yellow solid; yield, 78%; mp: 127-129 °C; ^{1}H NMR(400 MHz, $CDCl_3$) δ: 7.73 (s, 1H, CH=N), 7.36 (m, 1H, Ar-H), 7.20 (m, 1H, Ar-H). 7.13 (m, 1H, Ar-H). 6.71 (m, 1H, Ar-H), 4.94 (s, 2H, CH_2), 3.77 (s, 3H, N-CH_3), 3.60 (s, 3H, N-CH_3), 2.60 (q, J = 7.6 Hz, 2H, CH_2), 2.35 (s, 3H, CH_3), 1.22 (t, J = 7.6 Hz, 3H, CH_3). ^{13}C NMR (100 MHz, $CDCl_3$) δ: 149.4, 148.7, 147.1, 146.6, 141.0, 137.5, 135.1, 128.3, 124.2, 123.9, 120.6, 115.5, 109.1, 100.0, 99.9, 63.3, 37.4, 34.2, 19.4, 14.7, 13.0. HRMS (ESI) m/z calcd for $C_{20}H_{22}ClF_3N_5O_3$, 472.1363; found, 472.1364 $[M + H]^+$.

5-(4-Fluorophenoxy)-1-methyl-3-methyl-1H-pyrazole-4-carbaldehyde-O-{[4-chloro-3-(4-fluorophenyl)-1-methyl-1H-pyrazol-5-yl]methyl}oxime ***(10A)***. White solid; yield, 85%; mp: 133-134 °C; ^{1}H NMR (400 MHz, $CDCl_3$) δ: 7.85 (m, 2H, Ar-H), 7.77 (s, 1H, CH=N), 7.10 (m, 2H, Ar-H), 7.00 (m, 2H, Ar-H), 6.84 (m, 2H, Ar-H), 5.04 (s, 2H, CH_2), 3.88 (s, 3H, CH_3), 3.59 (s, 3H, CH_3), 2.36 (s, 3H, CH_3). ^{13}C NMR (100 MHz, $CDCl_3$) δ: 162.6, 158.8, 152.6, 152.5, 148.0, 147.1, 145.0, 141.6, 136.7, 128.9, 127.9, 116.6, 116.5, 116.4, 115.4, 108.4, 99.7, 63.3, 37.8, 34.3, 14.8. HRMS (ESI) m/z calcd for $C_{23}H_{21}ClF_2N_5O_2$, 472.1352; found, 472.1348 $[M + H]^+$.

5-(4-Chlorophenoxy)-1-methyl-3-methyl-1H-pyrazole-4-carbaldehyde-O-{[4-chloro-3-(4-fluorophenyl)-1-methyl-1H-pyrazol-5-yl]methyl}oxime ***(10B)***. White solid; yield, 85%; mp: 155-157 °C; ^{1}H NMR (400 MHz, $CDCl_3$) δ: 7.85 (m, 2H, Ar-H), 7.77 (s, 1H, CH=N), 7.26 (m, 2H, Ar-H), 7.10 (t, J =8.8 Hz, 2H, Ar-H), 6.82 (m, 2H, Ar-H), 5.04 (s, 2H, CH_2), 3.88 (s, 3H, CH_3), 3.58 (s, 3H, CH_3), 2.35 (s, 3H, CH_3). ^{13}C NMR (100 MHz, $CDCl_3$) δ: 162.6, 155.1, 147.5, 145.0, 141.4, 136.6, 130.0, 128.9, 116.6, 115.5, 108.4, 99.9, 63.3, 37.8, 34.3, 14.7. HRMS (ESI) m/z calcd for $C_{23}H_{21}Cl_2FN_5O_2$, 488.1056; found, 488.1043 $[M + H]^+$.

5-(4-Bromophenoxy)-1-methyl-3-methyl-1H-pyrazole-4-carbaldehyde-O-{[4-chloro-3-(4-fluorophenyl)-1-methyl-1H-pyrazol-5-yl]methyl}oxime ***(10C)***. White solid; yield, 83%; mp: 167-168 °C; ^{1}H NMR (400 MHz, $CDCl_3$) δ: 7.85 (m, 2H, Ar-H), 7.77 (s, 1H, CH=N), 7.41 (d, J = 8.6 Hz, 2H, Ar-H), 7.11 (m, 2H, Ar-H), 6.78 (d, J = 8.6 Hz, 2H, Ar-H), 5.04 (s, 2H, CH_2), 3.88 (s, 3H, CH_3), 3.58

(s, 3H, CH_3), 2.35 (s, 3H, CH_3). ^{13}C NMR (100 MHz, $CDCl_3$) δ: 162.6, 155.7, 147.3, 147.1, 145.0, 141.4, 136.6, 132.9, 128.9, 127.9, 127.8, 117.0, 116.3, 115.4, 108.4, 99.9, 63.3, 37.8, 34.3, 14.7. HRMS (ESI) m/z calcd for $C_{23}H_{21}BrClFN_5O_2$, 532.0551; found, 532.0538 $[M + H]^+$.

5-(4-Iodophenoxy)-1-methyl-3-methyl-1H-pyrazole-4-carbaldehyde-O-{[4-chloro-3-(4-fluorophenyl)-1-methyl-1H-pyrazol-5-yl]methyl}oxime ***(10D)***. White solid; yield, 84%; mp: 163-165 °C; ^{1}H NMR (400 MHz, $CDCl_3$) δ: 7.85 (q, J = 5,4 Hz, Ar-H), 7.77 (s, 1H, CH=N), 7.60 (d, J = 8.8 Hz, 2H, Ar-H), 7.11 (t, J = 8.8 Hz, 2H, Ar-H), 6.66 (d, J = 8.8 Hz, 2H, Ar-H), 5.04 (s, 2H, CH_2), 3.88 (s, 3H, CH_3), 3.58 (s, 3H, CH_3), 2.35 (s, 3H, CH_3). ^{13}C NMR (100 MHz, $CDCl_3$) δ: 162.6, 156.5, 147.3, 147.1, 145.0, 141.4, 138.9, 136.6, 128.9, 127.9, 127.9, 117.5, 115.4, 108.4, 99.9, 86.6, 63.3, 37.8, 34.3, 14.7. HRMS (ESI) m/z calcd for $C_{23}H_{21}IClFN_5O_2$, 580.0412; found, 580.0393 $[M + H]^+$.

5-(4-Methylphenoxy)-1-methyl-3-methyl-1H-pyrazole-4-carbaldehyde-O-{[4-chloro-3-(4-fluorophenyl)-1-methyl-1H-pyrazol-5-yl]methyl}oxime ***(10E)***. White solid; yield, 86%; mp: 136-138 °C; ^{1}H NMR (400 MHz, $CDCl_3$) δ: 7.84 (m, 2H, Ar-H), 7.78 (s, 1H, CH=N), 7.10 (m, 4H, Ar-H), 6.77 (d, J = 8.8 Hz, 2H, Ar-H), 5.05 (s, 2H, CH_2), 3.88 (s, 3H, CH_3), 3.57 (s, 3H, CH_3), 2.37 (s, 3H, CH_3), 2.30 (s, 3H, CH_3). ^{13}C NMR (100 MHz, $CDCl_3$) δ: 162.6, 154.6, 148.4, 146.9, 145.0, 141.9, 136.8, 133.3, 30.4, 128.9, 115.4, 115.1, 108.4, 99.7, 63.3, 37.8, 34.3, 20.6, 14.9. HRMS (ESI) m/z calcd for $C_{24}H_{24}ClFN_5O_2$, 468.1603; found, 468.1592 $[M + H]^+$.

5-(4-Methoxyphenoxy)-1-methyl-3-methyl-1H-pyrazole-4-carbaldehyde-O-{[4-chloro-3-(4-fluorophenyl)-1-methyl-1H-pyrazol-5-yl]methyl}oxime ***(10F)***. White solid; yield, 84%; mp: 127-129 °C; ^{1}H NMR (400 MHz, $CDCl_3$) δ: 7.84 (m, 2H, Ar-H), 7.76 (s, 1H, CH=N), 7.10 (t, J = 8.8 Hz, 2H, Ar-H), 6.82 (s, 4H, Ar-H), 5.06 (s, 2H, CH_2), 3.89 (s, 3H, CH_3), 3.76 (s, 3H, OCH_3), 3.60 (s, 3H, CH_3), 2.36 (s, 3H, CH_3). ^{13}C NMR (100MHz, $CDCl_3$) δ: 162.6, 155.8, 150.6, 148.7, 146.9, 145.0, 141.9, 136.8, 128.9, 128.0, 127.9, 116.3, 115.4, 115.0, 108.4, 99.5, 63.2, 55.7, 37.8, 34.3, 15.0. HRMS (ESI) m/z calcd for $C_{24}H_{24}ClFN_5O_3$, 484.1552; found, 484.1544 $[M + H]^+$.

5-(4-Trifluoromethoxyphenoxy)-1-methyl-3-methyl-1H-pyrazole-4-carbaldehyde-O-{[4-chloro-3-(4-fluorophenyl)-1-methyl-1H-pyrazol-5-yl]methyl}oxime ***(10G)***. White solid; yield, 86%; mp: 77-78 °C; ^{1}H NMR (400 MHz, $CDCl_3$) δ: 7.85 (m, 2H, Ar-H), 7.79 (s, 1H, CH=N), 7.17 (d, J = 8.8 Hz, 2H, Ar-H), 7.10 (t, J = 8.8 Hz , 2H, Ar-H), 6.90 (m, 2H, Ar-H), 5.03 (s, 2H, CH_2), 3.88 (s, 3H, CH_3), 3.60 (s, 3H, CH_3), 2.36 (s, 3H, CH_3). ^{13}C NMR (100 MHz, $CDCl_3$) δ: 162.6, 154.9, 147.4, 147.2, 145.0, 144.9, 141.4, 136.6, 128.9, 127.9, 127.8, 122.9, 120.4, 116.3, 115.4, 108.4, 99.9, 63.3, 37.8, 34.3, 14.7. HRMS (ESI) m/z calcd for $C_{24}H_{21}ClF_4N_5O_3$, 538.1269; found, 538.1256 $[M + H]^+$.

5-(4-Fluorophenoxy)-1-methyl-3-methyl-1H-pyrazole-4-carbaldehyde-O-{[4-chloro-3-(4-chlorophenyl)-1-methyl-1H-pyrazol-5-yl]methyl}oxime ***(10H)***. White solid; yield, 84%; mp: 126-128 °C; ^{1}H NMR (400 MHz, $CDCl_3$) δ: 7.83 (d, J = 8.4 Hz, 2H, Ar-H), 7.77 (s, 1H, CH=N), 7.39 (d, J = 8.4 Hz, 2H, Ar-H), 7.01 (m, 2H, Ar-H), 6.85 (m, 2H, Ar-H), 5.04 (s, 2H, CH_2), 3.89 (s, 3H, CH_3), 3.59 (s, 3H, CH_3), 2.35 (s, 3H, CH_3). ^{13}C NMR (100 MHz, $CDCl_3$) δ: 158.8, 152.6, 148.0, 147.1, 144.7, 141.6, 136.8, 133.9, 130.3, 128.6, 128.3, 116.7, 116.6, 116.5, 116.5, 108.6, 99.7, 62.4, 37.9, 34.3, 14.8. HRMS (ESI) m/z calcd for $C_{23}H_{21}Cl_2FN_5O_2$, 488.1056; found, 488.1048 $[M + H]^+$.

5-(4-Chlorophenoxy)-1-methyl-3-methyl-1H-pyrazole-4-carbaldehyde-O-{[4-chloro-3-(4-chlorophenyl)-1-methyl-1H-pyrazol-5-yl]methyl}oxime ***(10I)***. White solid; yield, 86%; mp: 100-102 °C; ^{1}H NMR (400 MHz, $CDCl_3$) δ: 7.83 (d, J = 8.4 Hz, 2H, Ar-H), 7.77 (s, 1H, CH=N), 7.38 (d, J = 8.8 Hz, 2H, Ar-H), 7.26 (t, J = 4.4 Hz, 2H, Ar-H), 6.82 (d, J = 9.2 Hz, 2H, Ar-H), 5.04 (s, 2H, CH_2), 3.88 (s, 3H, CH_3), 3.58 (s, 3H, CH_3), 2.35 (s, 3H, CH_3). ^{13}C NMR (100 MHz, $CDCl_3$) δ: 155.1, 147.4, 147.1, 144.6, 141.5, 136.8, 133.9, 130.3, 130.0, 128.9, 128.6, 128.3, 116.6, 108.6, 99.8, 63.3, 37.9, 34.3, 14.7. HRMS (ESI) m/z calcd for $C_{23}H_{21}Cl_3N_5O_2$, 504.0761; found, 504.0751 $[M + H]^+$.

5-(4-Bromophenoxy)-1-methyl-3-methyl-1H-pyrazole-4-carbaldehyde-O-{[4-chloro-3-(4-chlorophenyl)-1-methyl-1H-pyrazol-5-yl]methyl}oxime ***(10J)***. White solid; yield, 85%; mp: 116-118 °C; ^{1}H NMR (400 MHz, $CDCl_3$) δ: 7.83 (d, J = 8.4 Hz, 2H, Ar-H), 7.77 (s, 1H, CH=N), 7.40 (m, 4H, Ar-H), 6.77 (d, J = 8.4 Hz, 2H, Ar-H), 5.04 (s, 2H, CH_2), 3.88 (s, 3H, CH_3), 3.58 (s, 3H, CH_3), 2.35 (s, 3H, CH_3). ^{13}C NMR (100 MHz, $CDCl_3$) δ: 155.7, 147.3, 147.1, 144.7, 141.4, 136.8, 133.9, 133.0, 130.3, 128.6, 128.3, 117.0, 116.3, 108.6, 99.9, 63.3, 37.9, 34.3, 14.7. HRMS (ESI) m/z calcd for $C_{23}H_{21}BrCl_2N_5O_2$, 548.0256; found, 548.0242 $[M + H]^+$.

5-(4-Iodophenoxy)-1-methyl-3-methyl-1H-pyrazole-4-carbaldehyde-O-{[4-chloro-3-(4-chlorophenyl)-1-methyl-1H-pyrazol-5-yl]methyl}oxime ***(10K)***. White solid; yield, 83%; mp: 134-136 °C; ^{1}H NMR (400MHz, $CDCl_3$) δ: 7.83 (d, J = 8.8 Hz, 2H, Ar-H), 7.77 (s, 1H, CH=N), 7.60 (d, J = 8.8 Hz, 2H, Ar-H), 7.39 (d, J = 8.8 Hz, 2H, Ar-H), 6.66 (d, J = 9.2 Hz, 2H, Ar-H), 5.03 (s, 2H, CH_2), 3.88 (s, 3H, N-CH_3), 3.58 (s, 3H, N-CH_3), 2.35 (s, 3H, CH_3). ^{13}C NMR (100 MHz, $CDCl_3$) δ: 156.5, 147.3, 147.1, 144.7, 141.4, 138.9, 136.8, 133.9, 130.3, 128.6, 128.3, 117.5, 108.6, 99.9, 86.6, 63.3, 37.9, 34.3, 14.7. HRMS (ESI) m/z calcd for $C_{23}H_{21}ICl_2N_5O_2$, 596.0117; found, 596.0105 $[M + H]^+$.

5-(4-Methylphenoxy)-1-methyl-3-methyl-1H-pyrazole-4-carbaldehyde-O-{[4-chloro-3-(4-chlorophenyl)-1-methyl-1H-pyrazol-5-yl]methyl}oxime ***(10L)***. White solid; yield, 84%; mp: 111-112 °C; ^{1}H NMR (400 MHz, $CDCl_3$) δ: 7.82 (d, J = 8.8 Hz, 2H, Ar-H), 7.77 (s, 1H, CH=N), 7.38 (d, J = 8.4 Hz, 2H, Ar-H), 7.09 (d, J = 8.8 Hz, 2H, Ar-H), 6.76 (d, J = 8.4 Hz, 2H, Ar-H), 5.05 (s, 2H, CH_2), 3.88 (s, 3H, CH_3), 3.57 (s, 3H, CH_3), 2.36 (s, 3H, CH_3), 2.30 (s, 3H, CH_3). ^{13}C NMR (100 MHz, $CDCl_3$) δ: 154.6, 148.4, 146.9, 144.6, 141.9, 136.9, 133.8, 133.3, 130.4, 130.3, 128.6, 128.3, 115.1, 108.6, 99.7, 63.2, 37.9, 34.2, 20.6, 14.9. HRMS (ESI) m/z calcd for $C_{24}H_{24}Cl_2N_5O_2$, 484.1307; found, 484.1306 $[M + H]^+$.

5-(4-Methoxyphenoxy)-1-methyl-3-methyl-1H-pyrazole-4-carbaldehyde-O-{[4-chloro-3-(4-chlorophenyl)-1-methyl-1H-pyrazol-5-yl]methyl}oxime ***(10M)***. White solid; yield, 83%; mp: 109-111 °C; ^{1}H NMR (400 MHz, $CDCl_3$) δ: 7.82 (d, J = 8.4 Hz, 2H, Ar-H), 7.76 (s, 1H, CH=N), 7.38 (d, J = 8.8 Hz, 2H, Ar-H), 6.82 (s, 4H, Ar-H), 5.05 (s, 2H, CH_2), 3.89 (s, 3H, CH_3), 3.76 (s, 3H, OCH_3), 3.58 (s, 3H, CH_3), 2.35 (s, 3H, CH_3). ^{13}C NMR (100 MHz, $CDCl_3$) δ: 155.8, 150.6, 148.7, 146.9, 144.6, 141.9, 136.9, 133.8, 130.3, 128.6, 128.4, 116.3, 115.0, 108.6, 99.5, 63.2, 55.7, 37.9, 34.2, 14.9. HRMS (ESI) m/z calcd for $C_{24}H_{24}Cl_2N_5O_3$, 500.1256; found, 500.1247 $[M + H]^+$.

*5-(4-Trifluoromethoxyphenoxy)-1-methyl-3-methyl-1H-pyrazole-4-carbaldehyde-O-{[4-chloro-3-(4-chlorophenyl)-1-methyl-1H-pyrazol-5-yl]methyl}oxime (**10N**).* White solid; yield, 85%; mp: 85-86 °C; ^{1}H NMR (400 MHz, $CDCl_3$) δ: 7.83 (d, J = 8.8Hz, 2H, Ar-H), 7.78 (s, 1H, CH=N), 7.38 (d, J = 8.4 Hz, 2H, Ar-H), 7.17 (d, J = 8.8 Hz, 2H, Ar-H), 6.90 (d, J = 9.2 Hz, 2H, Ar-H), 5.03 (s, 2H, CH_2), 3.88 (s, 3H, CH_3), 3.60 (s, 3H, CH_3), 2.36 (s, 3H, CH_3). ^{13}C NMR (100 MHz, $CDCl_3$) δ: 154.8, 147.4, 147.1, 144.7, 141.4, 136.7, 133.9, 130.3, 128.6, 128.3, 122.9, 116.3, 108.6, 99.9, 63.3, 37.8, 34.8, 14.7. HRMS (ESI) m/z calcd for $C_{24}H_{21}Cl_2F_3N_5O_3$, 554.0974; found, 554.0962 $[M + H]^+$.

4.2. Cell culture and reagents

Human hepatocellular carcinoma cells (SMMC-7721), human gastric cancer cells (SGC7901), human colon cancer cells (HCT116) and human liver normal cells (LO2) were maintained in DMEM supplemented with 10% fetal bovine serum (Invitrogen), 100 units/ml of penicillin, and 0.1 µg/ml of streptomycin in a humid atmosphere incubator with 5% CO_2 at 37 °C. All cell lines were originally from the Shanghai Institute of Cell Biology (Shanghai, China). Cells were routinely subcultured twice weekly. 3-(4,5-dimethylthiazol-2-yl)-2,5-diphenyltetrazolium bromide (MTT), monoclonal anti-actin antibody, and goat peroxidase-conjugated anti-rabbit IgG antibody, and goat peroxidase-conjugated anti-mouse IgG antibody were purchased from Sigma-Aldrich (St. Louis, MO). FITC-Annexin V and PI are from (BioVision). Antibodies such as Bax, Bcl-2, p-H2AX, cleaved-PARP, cleaved-caspase 3, and p-p53 (S15) are from Cell Signaling Technology (Danvers, MA).

4.3. MTT assay

Anti-proliferative activities of synthesized compounds were evaluated *in vitro* against three human cancer cell lines (SMMC-7721, SGC7901, and HCT116) and human normal cell (LO2). Briefly, 100 µL of different cells were plated in a 96-well flat bottom tissue culture plate at a density of 10^4 cells/mL, respectively, in DMEM medium and 10% fetal bovine serum and allowed to adhere overnight at 37 °C in 5% CO_2. The cells were incubated in triplicate with, or without, different concentrations of each test compound for 72 h. During the last 4 h incubation, 30 µL of tetrazolium dye (MTT) solution (5 mg/mL) was added to each well. The resulting MTT-formazan crystals were dissolved in 150 µL DMSO, and absorbance was measured spectrophotometrically at 570 nm using an ELISA plate reader. The inhibition induced by each test compound at the indicated concentrations was expressed as a percentage. The concentration required for 50% inhibition (IC_{50}) was calculated using the software (GraphPadPrism Version 4.03).

4.4. Flow cytometry assay of cell apoptosis

SMMC-7721 cells were cultured overnight and incubated in triplicate with different concentrations of **10M**, ADM, or vehicle for 72 h. The cells were harvested and stained with APC-Annexin V and 7-AAD at room temperature for 15 min. The percentage of apoptotic cells was determined by flow cytometry (Calibur, BD, USA) analysis. The APC signal detector (FL4) (Ex = 633 nm; Em = 660 nm) and 7-AAD staining signal detector (FL3) (Ex = 488 nm; Em =647 nm) were used to detect the cells with the flow cytometer. Ten thousand cells were counted for three independent experiments. The data were analyzed using WinList 3D (version7.1) and the histogram was plotted using Excel 2010.

4.5. Western blot analysis

SMMC-7721 cells with or without ADM, or **10M** treatment at indicated time and doses were washed with PBS and lysed on ice for 30 minutes in PBS containing 1% Nonidet P-40, 0.5% sodium deoxycholate, 0.1% SDS, 10 mg/ml PMSF, and 20 mM leupeptin. The protein concentrations were determined using a Bio-Rad protein assay kit (Bio-Rad Laboratories Inc., Hercules, CA, USA). Up to 50 µg of total protein were separated onto an SDS-PAGE and transferred to polyvinylidenedifluoride membranes. After blocking with 5% fat free milk for 2 h, membranes were incubated overnight at 4 °C with a primary antibody in TBS-T and then reacted with a peroxidase-conjugated secondary antibody for 1 h. Immuno reactive proteins were detected with the ECL Western Blotting Detection System.

4.6. Maximum tolerated dose determination

All *in vivo* studies were approved by the Nantong University Animal Care and Use Committee. The maximum tolerated dose (MTD) of compound **10M** in female ICR mice were determined by intraperitoneal injection of a single dose of **10M** (488.3, 390.6, 312.5, 250, and 200 mg/kg) or vehicle control (n = 10 per group), respectively. The MTD was set below the dose that caused severe loss of body weight (>20% of original weight), or death of one or more animals of a dose group. MTD was defined as the highest dose that could be given resulting in no drug-related moribund state or death, while temporary body weight loss was within 20%.

4.7. In vivo tumor growth inhibition

Female BALB/c nude mice at the age of 5 to 6-week-old were inoculated subcutaneously with 10^6 SMMC-7721 cells. When tumor volumes reached 50-100 mm^3, the mice were randomly administered with **10M**, ADM, and vehicle, respectively. The body weight of all animals was monitored throughout the study and animals were euthanized if they incurred 20 % weight loss between observations. Two axes (mm) of a tumor (L, longest axis; W, shortest axis) were measured with a Vernier caliper. Tumor volume (mm^3) was calculated using a formula of "tumor volume = ½ ($L \times W^2$)". Progression of tumors was monitored every 3 days up to 19 days post treatment. At the end of the experiment, the mice were sacrificed, and their tumors were dissected out and weighed.

Acknowledgments

We gratefully acknowledge the financial support by the Natural Science Foundation of China (Grant Nos. 21372135 and 81302628), the Project of "Jiangsu Six Peaks of Talent" (2013-SWYY-013, 2014-SWYY-044, and 2016-SWYY-CXTD-008), China Pharmaceutical University for the Open Project Program of State Key Laboratory of Natural Medicines (SKLNMKF201611), China and Jiangsu Province Postdoctoral Science Foundation (2016M590488 and 1601136B), the Project

of "Jiangsu 333 high-level talents", Jiangsu Government Scholarship for Overseas Studies (JS-2014-212), Applied Research Projects of Nantong City (MS22015020, MS12015060), and also thank a project funded by the Priority Academic Programs Development of Jiangsu Higher Education Institutions (PAPD).

References and notes

[1] B.W. Stewart, C.P. Wild (Eds.), World Cancer Report 2014, vol. 3, International Association of Cancer Research, Lyon, France, 2014.
[2] H.P. Varbanov, F. Kuttler, D. Banfi, G. Turcatti, P.J. Dyson, repositioning approved drugs for the treatment of problematic cancers using a screening approach, Plos One. 12 (2017) e0171052.
[3] V.G. Reddy, T.S. Reddy, V.L. Nayak, B. Prasad, A.P. Reddy, A. Ravikumar, S. Taj, A. Kamal, Design, synthesis and biological evaluation of N-((1-benzyl-1*H*-1,2,3-triazol-4-yl)methyl)-1,3-diphenyl-1H-pyrazole-4-carboxamides as CDK1/Cdc2 inhibitors, Eur. J. Med. Chem. 122 (2016) 164-177.
[4] H.H. Gong, D. Addla, J.S. Lv, C.H. Zhou, Heterocyclic naphthalimides as new skeleton structure of compounds with increasingly expanding relational medicinal applications, Curr. Top. Med. Chem. 16 (2016) 3303-3364.
[5] Y. Ling, C. Xu, L. Luo, J. Cao, J. Feng, Y. Xue, Q. Zhu, C. Ju, F. Li, Y. Zhang, Y. Zhang, X. Ling, Novel beta-carboline/hydroxamic acid hybrids targeting both histone deacetylase and DNA display high anticancer activity via regulation of the p53 signaling pathway, J. Med. Chem. 58 (2015) 9214-9227.
[6] X. Zhao, Q. Tan, Z. Zhang, Y. Zhao, 1,3,5-Triazine inhibitors of histone deacetylases: synthesis and biological activity, Med. Chem. Res. 23 (2014) 5188-5196.
[7] A.A. Bekhit, H.M. Abdel-Rahman, A.A. Guemei, Synthesis and biological evaluation of some hydroxypyrazole derivatives as anti-inflammatory antimicrobial agents, Arch. Pharm. 339 (2006) 81-87.
[8] O.I. El-Sabbagh, M.M. Baraka, S.M. Ibrahim, C. Pannecouque, G. Andrei, R. Snoeck, J. Balzarini, A.A. Rashad, Synthesis and antiviral activity of new pyrazole and thiazole derivatives, Eur. J. Med. Chem. 44 (2009) 3746-3753.
[9] I. Koca, A. Ozgur, K.A. Coskun, Y. Tutar, Synthesis and anticancer activity of acyl thioureas bearing pyrazole moiety, Bioorg. Med. Chem. 21 (2013) 3859-3865.
[10] Y. Li, H.Q. Zhang, J. Liu, X.P. Yang, Z.J. Liu, Stereoselective synthesis and antifungal activities of (*E*)-alpha-(methoxyimino) benzeneacetate derivatives containing 1,3,5-substituted pyrazole ring, J. Agric. Food. Chem. 54 (2006) 3636-3640.
[11] P.C. Lv, H.Q. Li, J. Sun, Y. Zhou, H.L. Zhu, Synthesis and biological evaluation of pyrazole derivatives containing thiourea skeleton as anticancer agents, Bioorg. Med. Chem. 18 (2010) 4606-4614.
[12] S.G. Alegaon, M.B. Hirpara, K.R. Alagawadi, S.S. Jalalpure, V.P. Rasal, P.S. Salve, V.M. Kumbar, Synthesis and biological evaluation of 1,3,4-trisubstituted pyrazole analogues as anti-mycobacterial agents, Med. Chem. Res. 26 (2017) 1127-1138.
[13] P. Kundu, N. Chattopadhyay, Interaction of a bioactive pyrazole derivative with calf thymus DNA: Deciphering the mode of binding by multi-spectroscopic and molecular docking investigations, J. Photochem. Photobiol. B, Biol. 173 (2017) 485-492.
[14] M.G. Prabhudeva, S. Bharath, A.D. Kumar, S. Naveen, N.K. Lokanath, B.N. Mylarappa, K.A. Kumar, Design and environmentally benign synthesis of novel thiophene appended pyrazole analogues as anti-inflammatory and radical scavenging agents: Crystallographic, in silico modeling, docking and SAR characterization, Bioorg. Chem. 73 (2017) 109-120.
[15] Y. Wang, F.X. Cheng, X.L. Yuan, W.J. Tang, J.B. Shi, C.Z. Liao, X.H. Liu, Dihydropyrazole derivatives as telomerase inhibitors: structure-based design, synthesis, SAR and anticancer evaluation in vitro and in vivo, Eur. J. Med. Chem. 112 (2016) 231-251.
[16] Y.Y. Chen, X.Q. Wu, W.J. Tang, J.B. Shi, J. Li, X.H. Liu, Novel dihydropyrazole-chromen: design and modulates hTERT inhibition proliferation of MGC-803, Eur. J. Med. Chem. 110 (2016) 65-75.
[17] V.G. Reddy, T.S. Reddy, V.L. Nayak, B. Prasad, A.P. Reddy, A. Ravikumar, S. Taj, A. Kamal, Design, synthesis and biological evaluation of N-((1-benzyl-1H-1,2,3-triazol-4-yl)methyl)-1,3–diphenyl-1*H*-pyrazole-4-carboxamides as CDK1/CDC2 inhibitors, Eur. J. Med. Chem. 122 (2016) 164-177.
[18] J. Sun, X.H. Lv, H.Y. Qiu, Y.T. Wang, Q.R. Du, D.D. Li, Y.H. Yang, H.L. Zhu, Synthesis, biological evaluation and molecular docking studies of pyrazole derivatives coupling with a thiourea moiety as novel CDKs inhibitors, Eur. J. Med. Chem. 68 (2013) 1-9.
[19] A.S. Hassan, M.F. Mady, H.M. Awad, T.S. Hafez, Synthesis and antitumor activity of some new pyrazole 1,5-a pyrimidines, Chin. Chem. Lett. 28 (2017) 388-393.
[20] X.L. Ding, N. Meng, Y. Xia, L.J. Wang, X.F. Zhang, B.X. Zhao, J.Y. Miao, Synthesis and bioactivity evaluation of ethyl 1-arylmethyl-3-aryl-1-H-pyrazole-5- carboxylate derivatives, Chin. J. Org. Chem. 27 (2007) 1542-1546.
[21] C.L. Chen, J. Chen, H. Gu, N. Bao, H. Dai, Design, synthesis, and biological activities of novel pyrazole oxime compounds containing a substituted pyridyl moiety, Molecules, 22 (2017) 878-892.
[22] H. Dai, Y.Q. Li, D. Du, X. Qin, X. Zhang, H.B. Yu, J.X. Fang, Synthesis and biological activities of novel pyrazole oxime derivatives containing a 2-chloro-5-thiazolyl moiety, J. Agric. Food Chem. 56 (2008) 10805-10810.
[23] G.P. Lahm, T.P. Selby, J.H. Freudenberger, T.M. Stevenson, B.J. Myers, G. Seburyamo, B.K. Smith, L. Flexner, C.E. Clark, D. Cordova, Insecticidal anthranilic diamides: A new class of potent ryanodine receptor activators, Bioorg. Med. Chem. Lett. 15 (2005) 4898-4906.
[24] S. Fustero, R. Roman, J.F. Sanz-Cervera, A. Simon-Fuentes, A.C. Cunat, S. Villanova, M. Murguia, Improved regioselectivity in pyrazole formation through the use of fluorinated alcohols as solvents: Synthesis and biological activity of fluorinated Tebufenpyrad analogs, J. Org. Chem. 73 (2008) 3523-3529.
[25] S. Fustero, R. Roman, J.F. Sanz-Cervera, A. Simon-Fuentes, J. Bueno, S. Villanova, Synthesis of new fluorinated Tebufenpyrad analogs with acaricidal activity through regioselective pyrazole formation, J. Org. Chem. 73 (2008) 8545-8552.
[26] X.H. Liu, L.P. Zhi, B.A. Song, H.L. Xu, Synthesis, characterization and antibacterial activity of new 5-aryl pyrazole oxime ester derivatives, Chem. Res. Chin. Univ. 24 (2008) 454-458.
[27] A.V. Gadakh, C. Pandit, S.S. Rindhe, B.K. Karale, Synthesis and antimicrobial activity of novel fluorine containing 4-(substituted-2-hydroxybenzoyl)-1H-pyrazoles and pyrazolyl benzodoxazoles, Bioorg. Med. Chem. Lett. 20 (2010) 5572-5576.
[28] C. Fu, J. Pei, Y. Ning, M. Liu, P. Shan, J. Liu, Y. Li, F. Hu, Y. Zhu, H. Yang, X. Zou, Synthesis and insecticidal activities of novel pyrazole oxime ether derivatives with different substituted pyridyl rings, Pest. Manag. Sci. 70 (2014) 1207-1214.
[29] T.S. Reddy, H. Kulhari, V.G. Reddy, V. Bansal, A. Kamal, R. Shukla, Design, synthesis and biological evaluation of 1,3-diphenyl-1H-pyrazole derivatives containing benzimidazole skeleton as potential anticancer and apoptosis inducing agents, Eur. J. Med. Chem. 101 (2015) 790-805.
[30] M. Riga, A. Myridakis, D. Tsakireli, E. Morou, E.G. Stephanou, R. Nauen, T. Van Leeuwen, V. Douris, J. Vontas, Functional characterization of the Tetranychus urticae CYP392A11, a cytochrome P450 that hydroxylates the METI acaricides cyenopyrafen and fenpyroximate, Insect. Biochem. Molec. 65 (2015) 91-99.
[31] L. Lopez, H.A. Smith, M.A. Hoy, J.R. Bloomquist, Acute toxicity and sublethal effects of Fenpyroximate to Amblyseius swirskii (Acari: Phytoseiidae), J. Econ. Entomol. 108 (2015) 1047-1053.
[32] D.B. Lima, J.W.S. Melo, M.G.C. Gondim, Jr., R.N.C. Guedes, J.E.M. Oliveira, Population-level effects of abamectin, azadirachtin and fenpyroximate on the predatory mite Neoseiulus baraki, Exp. Appl. Acarol. 70 (2016) 165-177.
[33] H.J. Park, K. Lee, S.J. Park, B. Ahn, J.C. Lee, H. Cho, K.I. Lee, Identification of antitumor activity of pyrazole oxime ethers, Bioorg. Med. Chem. Lett. 15 (2005) 3307-3312.
[34] H. Dai, S.S. Ge, G. Li, J. Chen, Y.J. Shi, L.Y. Ye, Y. Ling, Synthesis and bioactivities of novel pyrazole oxime derivatives containing a 1,2,3-

thiadiazole moiety, Bioorg. Med. Chem. Lett. 26 (2016) 4504-4507.
[35] S.M. Gomha, T.A. Farghaly, A.R. Sayed, M.M. Abdalla, Synthesis of pyrazolyl pyrazoles and pyrazolyl-1,2,4-triazolo-3,4-d-1,5-benzothiazepines as p53 activators using hydrazonoyl chlorides, J. Heterocycl. Chem. 53 (2016) 1505-1511.
[36] F. Wei, B.X. Zhao, B. Huang, L. Zhang, C.H. Sun, W.L. Dong, D.S. Shin, J.Y. Miao, Design, synthesis, and preliminary biological evaluation of novel ethyl 1-(2'-hydroxy-3'-aroxypropyl)-3-aryl-1H-pyrazole-5-carboxylate, Bioorg. Med. Chem. Lett. 16 (2006) 6342-6347.
[37] M.S. Park, H.J. Park, K.H. Park, K.I. Lee, Introduction of N-containing heterocycles into pyrazole by nucleophilic aromatic substitution, Synth. Commun. 34 (2004) 1541-1550.
[38] H. Dai, G. Li, J. Chen, Y.J. Shi, S.S. Ge, C.G. Fan, H.B. He, Synthesis and biological activities of novel 1,3,4-thiadiazole-containing pyrazole oxime derivatives, Bioorg. Med. Chem. Lett. 26 (2016) 3818-3821.
[39] T. Harada, K. Harada, Y. Ueyama, The enhancement of tumor radioresponse by combined treatment with cepharanthine is accompanied by the inhibition of DNA damage repair and the induction of apoptosis in oral squamous cell carcinoma, Int. J. Oncol. 41 (2012) 565-572.
[40] A. Sharma, K. Singh, A. Almasan, Histone H2AX phosphorylation: a marker for DNA damage, Methods. Mol. Biol. 920 (2012) 613-626.
[41] H.B. Lieberman, S.K. Panigrahi, K.M. Hopkins, L. Wang, C.G. Broustas, p53 and RAD9, the DNA damage response, and regulation of transcription networks, Radiat. Res. 187 (2017) 424-432.

Supplementary Material

Supplementary material that may be helpful in the review process should be prepared and provided as a separate electronic file. That file can then be transformed into PDF format and submitted along with the manuscript and graphic files to the appropriate editorial off

Click here to remove instruction text...

Development of novel bis-pyrazole derivatives as antitumor agents with potent apoptosis induction effects and DNA damage

Hong Dai [a,b], Shushan Ge [a,b], Jin Guo [b,c], Shi Chen [b,c], Meiling Huang [b], Jiaying Yang [b], Siyu Sun [a], Yujun Shi [a,*], and Yong Ling [a,b,c,*]

[a] College of Chemistry and Chemical Engineering, Nantong University, Nantong 226019, People's Republic of China

[b] School of Pharmacy, Nantong University, Nantong 226001, People's Republic of China

[c] Jiangsu Province Key Laboratory for Inflammation and Molecular Drug Target, Nantong University, Nantong 226001, China.

Highlights

- New bis-pyrazole derivatives were designed and synthesized.
- Compound **10M** selectively inhibited cancer cells but not non-tumor cell.
- **10M** trigged cancer cell apoptosis by cleavage of caspase 3 and PARP.
- **10M** induced DNA damage by activation of the p53 signaling pathway.
- **10M** showed low acute toxicity and significant tumor growth inhibition *in vivo*.